University of Alberta
Department of Civil Engineering

Structural Engineering Report No. 98

Design Methods for Steel Box-Girder Support Diaphragms

by

Robert J. Ramsay

and

Reidar Bjorhovde

July, 1981

Structural Engineering Report No. 98

DESIGN METHODS FOR STEEL BOX-GIRDER SUPPORT DIAPHRAGMS

by

Robert J. Ramsay

and

Reidar Bjorhovde

Department of Civil Engineering
University of Alberta
Edmonton, Alberta, Canada

July, 1981

ABSTRACT

The behavior of steel support diaphragms in box girders is complex and cannot be adequately described by simple analytical methods. As a result semi-empirical procedures are often used for their design. This study evaluates three such procedures and comments on their adequacy. Also, simple rules are developed to ensure an efficient diaphragm design.

LIST OF FIGURES

TABLE OF CONTENTS

1. INTRODUCTION

Steel box girders have the advantage of not only being efficient in bending and torsion, but also of being aesthetically pleasing. As a result they have been extensively used as components of bridge superstructures.

The behavior of steel box girders is similar in many respects to that of steel plate girders. Design rules which cover the behavior of plate girders can often be extrapolated to cover the behavior of box girders. However there are several fundamental differences between the behavior characteristics of these types of girders, which must be taken into account in a rational design approach.

One of the most important of the unique features of box girders is the manner in which the vertical loads are transferred from the girder webs to the bearings. This is illustrated in Figure 1. In plate girders these loads are transferred directly to the bearing through bearing stiffeners acting as struts. In box girders the bearings are not commonly located directly beneath the webs, and the vertical loads must be transferred from the webs to the bearing through a diaphragm. This creates a complex state of stress in the diaphragm. Thus, vertical stresses are present due to the vertical loads, while horizontal and shear stresses are present due to the beam action of the diaphragm spanning over the bearing.

Traditionally, support diaphragms were designed as perfectly straight and initially stress free elastic plates.[1] The strength of the slender plates after buckling was ignored, and the capacity was

based on the elastic buckling strength. It was felt that in actual structures the post-buckling reserve strength would compensate for the weakening effects of geometric imperfections and residual stresses. However, for plates with the relatively small slendernesses typical of those used in bridge support diaphragms, the post-buckling reserve strength is small, whereas the weakening effects due to geometric imperfections and residual stresses are not.

In June, 1970, a steel box girder bridge under erection at Milford Haven, Wales, collapsed due to failure of the pier support diaphragm.[2] The subsequent inquiry revealed that not only was the diaphragm out of flat by 3/4 inch, but also that it was not correctly centered over the bearing. These effects subjected the diaphragm to out-of-plane bending moments for which it was not designed.

As a result of this and other box girder failures, the British Government set up a committee to establish rules to govern the design and construction of box girders. These rules were subsequently named the "Interim Design Rules"[3] or the "Merrison Report" after the name of the committee chairman and placed considerable emphasis on the weakening effects of geometric imperfections and residual stresses. Unfortunately, the rules were also quite complex, and the resulting designs tended to be overly conservative at times.

Subsequent work has been done at the Transport and Road Research Laboratory in England,[4] to formulate (within the context of the Design Rules) simpler and less conservative rules for the design of support diaphragms. In North America, Wolchuk and Mayrbaurl proposed rules for the design of all components of steel box girder

bridges, including support diaphragms.[5]

Since the advent of the Interim Design Rules, the design of support diaphragms has been conservative due to the lack of understanding of their behavior. As a result, heavily stiffened diaphragms which are expensive to fabricate, due to the large amount of labor involved in installing the stiffeners, have become the norm in bridge construction.

2. SCOPE OF STUDY

Most steel box girder bridges can be classified into two categories,[2] as follows:

(1) Long span bridges composed of a single steel box supported on twin bearings, with a composite steel-concrete or an orthotropic steel deck, as shown in Figure 2a.

(2) Short to medium span bridges, composed of several steel boxes connected by external diaphragms at the supports, and having a composite steel-concrete deck, as shown in Figure 2b.

This study will examine the behavior of support diaphragms for the second type of bridge only, as this type has been used almost exclusively in North America. The support diaphragms are assumed to be rectangular or mildly trapezoidal (webs make an angle of less than 30° with the vertical) in shape.

Although diaphragms with inspection manholes are commonly used in bridges, the resulting complexities in behavior are considered beyond the scope of this study. The holes are typically placed in a lightly stressed area of the diaphragm, i.e. near the top of the diaphragm, directly over the bearing, and surrounded by stiffeners. Diaphragms supported on a single bearing and with twin load-bearing stiffeners may have the stiffeners placed in a V shape, allowing a larger manhole to be used. Despite these precautions, the manhole is often the weakest link in the diaphragm system, and should be the topic of additional research.

Steel box girders often have intermediate diaphragms in addition

to support diaphragms. Their primary function is to reduce distortion of the girder cross-section, along with the accompanying longitudinal and transverse stresses. In addition, they provide extra stiffness to the box girder during construction before the deck is placed. Intermediate diaphragms are not as heavily loaded as support diaphragms, and are often constructed as cross frames rather than solid plates. For this reason they are not included in this study.

3. BEHAVIOR OF SUPPORT DIAPHRAGMS

3.1 Loads on Support Diaphragms

In general, support diaphragms may be subjected to vertical loads, horizontal loads acting perpendicular to the plane of the diaphragm, and horizontal loads acting in the plane of the diaphragm.

The vertical loads acting on the diaphragm are due to the weight of the bridge superstructure and the bridge traffic. They are transferred to the diaphragm through the girder webs, and can be seperated into symmetric and anti-symmetric components, as illustrated in Figure 3. For typical box girder geometries and spacings, the symmetric component of load produces larger moments and shears in the diaphragm than does the anti-symmetric component. Under symmetric loading the points of contraflexure in the diaphragm are near the locations of the webs. As a result, the internal diaphragm is subjected to a distribution of moments similar to that which would exist if the external diaphragms were not present. The anti-symmetric component of load results from torsion in the box girder, and is resisted by the external diaphragm spanning between adjacent boxes. If the box girder webs are sloped, there will be a horizontal as well as a vertical component to the shear force in the web. This component of shear produces horizontal loads in the diaphragm.

Horizontal loads acting perpendicular to the plane of the diaphragm are caused by longitudinal traffic forces, wind, girder length changes due to temperature effects at fixed bearings, and friction forces at expansion bearings. These loads produce out-of-plane

bending moments in the diaphragm. If the support diaphragm is not directly centered over the bearing due to construction misalignments or temperature movement, the resultant eccentric bearing reaction will cause an additional bending moment in the diaphragm. It will be recalled that this was one of the primary causes for the Milford Haven bridge failure. Diaphragm stiffening is required to resist these large out-of-plane moments.

Horizontal loads acting in the plane of the diaphragm are caused by creep and shrinkage strains in the concrete deck, by lateral temperature movements being resisted by the bearings, and by wind action. The horizontal forces due to creep, shrinkage and temperature movement, can be reduced if some of the bearings are allowed to move in the lateral direction. The horizontal loads produce axial forces and bending moments in the diaphragm.

3.2 Experimental Behavior of Support Diaphragms

Experimental research on the behavior of support diaphragms has been conducted at Imperial College and the Transport and Road Research Laboratory in England.[6,7,8] This work covered a number of types of diaphragms, ranging from unstiffened, rectangular diaphragms, to orthogonally stiffened, trapezoidal diaphragms. The diaphragms tested were loaded by concentric vertical loads applied to the girder webs. No horizontal loads were applied. This section will summarize the research results which are most relevant to multi-box girder systems, of the type shown in Figure 2b.

Support diaphragms behave elastically at low to moderate loads.

However, yielding can occur adjacent to the bearing, due to stress concentrations caused by bending of the diaphragm over the bearing and construction misalignments of the bearing surfaces. In addition, the diaphragm plate and stiffeners are not fabricated perfectly flat, due to fabrication tolerances. This results in the diaphragm deforming out-of-plane as soon as load is applied.

At increased loads the yielded portion of the diaphragm expands upward and outward from the bearing towards the web, as illustrated in Figure 4.[8] The size of the yielded zone at failure depends on the slenderness ratios of the stiffeners, and of the plate panels bounded by the stiffeners, webs and flanges. Naturally, stocky diaphragms are likely to have larger yielded zones at failure than slender ones.

There are several different mechanisms by which a support diaphragm can fail. For typical box girder diaphragms, these failure mechanisms all involve inelastic buckling.

Figure 5 shows a typical collapse mechanism for an unstiffened support diaphragm. Buckling action commences at a distance of approximately one-third of the total diaphragm depth above the bearing. The presence of the box girder bottom flange provides a stabilizing effect through rotational restraint of the base of the diaphragm.

The mechanism causing failure of support diaphragms with load-bearing stiffeners is governed by the stiffener size. For light stiffeners the failure mechanism is similar to the one causing failure in unstiffened diaphragms. Failure now not only involves buckling of the plate, but also buckling of the load-bearing stiffeners. Stiffener failure may be due to either flexural or torsional (twisting of the

stiffener while the diaphragm plate remains flat) buckling. For heavy stiffeners, buckling of the plate occurs with the load-bearing stiffeners remaining straight. The resulting failure mechanism is shown in Figure 6.

Support diaphragms with orthogonal stiffening show more complex behavior than that described for unstiffened or vertically stiffened diaphragms. Initial inelastic buckling of the diaphragm is confined to individual plate panels, and redistribution of load between panels is possible. At higher loads, buckling of the intermediate stiffeners between panels allows the formation of an overall failure mechanism. It is similar to that of an unstiffened diaphragm.

An alternate load path for carrying loads from the girder webs to the bearing is provided by the box girder bottom flange. For heavily stiffened flanges the percentage of load carried in this fashion can be as high as 30% of the total. The effect of this destabilizing force in a critical area of the flange requires further study.

The state of stress in a loaded support diaphragm is complex, and includes in-plane vertical, horizontal and shear stresses, in addition to out-of-plane bending stresses. This stress state is described briefly in the following paragraphs.

The vertical stresses in a support diaphragm are due to both axial load and out of plane bending moment. The distribution of vertical stresses across the width of the diaphragm due to axial load is shown in Figure 7b. The stresses decrease to zero at the webs, due to shear lag, and are at a maximum over the bearing.[8] The vertical stresses due to out of plane bending moment are resisted by the load-bearing stiffeners, and are distributed linearly over their depth.

Vertical stresses over the bearing are larger at the edges of the bearing than at the center, due to bending action of the diaphragm.

Support diaphragms are also subjected to horizontal stresses, due to deep beam action of the diaphragm in spanning over the bearing. Their distribution over the diaphragm depth is shown in Figure 7c. The sloping webs of trapezoidal diaphragms generate horizontal compressive forces in addition to those due to bending action. Due to Poisson's effect, the longitudinal stresses in the box girder flanges will reduce these compressive stresses. The simultaneous presence of both vertical and horizontal compressive stresses in the lower regions of the diaphragm causes destabilization of this critical area. However, it is possible to strengthen the diaphragm by using horizontal stiffeners.

Transfer of the vertical loads from the girder webs to the bearing is effected by shear stresses in the diaphragm. If the horizontal distance between the web and bearing is small, the distribution of shear over the depth will be as shown in Figure 7d. This peak becomes less pronounced as the distance between web and bearing increases. If shear is carried by tension field action in the web, the distribution of shear transmitted to the diaphragm will be altered, as shown by the dashed line in Figure 7d, due to the action of the web hanging off the top of the diaphragm.

With the exception of load-bearing stiffeners, diaphragm stiffeners are usually not highly stressed. However, horizontal stiffeners near the bottom of trapezoidal diaphragms can become highly stressed if the surrounding plate buckles.

3.3 Theoretical Prediction of Support Diaphragm Behavior

The prediction of support diaphragm behavior involves the analysis of the interaction between instability and plastic deformation in stiffened plates. Because of the plastic deformations, elastic buckling solutions can not be used directly to predict diaphragm capacity.

To solve this problem, Crisfield and Puthli[9,10] developed a finite element program which takes into account both geometric and material nonlinearities. The program can not take into account local stiffener buckling.

The model analysed by the finite element program consisted of a diaphragm with adjacent portions of web and flanges, as shown in Figure 8. The flange was assumed to be cut along lines of zero transverse shear. Three-dimensional analyses of the box girder region over the support have indicated that this is a conservative assumption.[11]

The diaphragm can be assumed to be either simply supported or restrained at its boundaries, i.e. at webs and flanges. Three dimensional finite element analyses have also shown that the box girder flanges will not destabilize the diaphragm, and a lower bound solution will be obtained by assuming simply supported edges.[11]

The accuracy of the results obtained from the finite element program have been verified through comparisons with experimental results for unstiffened diaphragms, and for diaphragms with load-bearing stiffeners only.[9,10] Comparisons have not been made with orthogonally stiffened diaphragms, because of the amount of computer capacity required for the analysis. In the comparisons between theoretical and experimental results, the geometric imperfections of the diaphragm plates and

stiffeners were represented as the sine waves which best fit the actual imperfections. Residual stresses were not taken into account.

The experimental collapse loads obtained from the diaphragm tests were in all cases bounded by the finite element results which assumed simply supported and restrained boundary conditions for the diaphragms. One of the major limitations in predicting accurate diaphragm failure loads therefore is the ability to predict diaphragm boundary conditions. The finite element program was also able to predict the proper failure mechanisms for the test diaphragms. Comparisons between experimental and theoretical stresses for vertical, horizontal and shear stresses in the diaphragm plates and vertical stresses in the load-bearing stiffeners are given in Reference 8. The comparisons are good considering the complexity of the problem.

The finite element program was used to conduct parametric studies on support diaphragms with load bearing stiffeners.[9,10] The parameters studied were the diaphragm width and depth, the offset of the girder web from the bearing, and the stiffener depth. The effects of geometric imperfections and eccentric loading were considered in the analyses, but the effect of residual stresses was not.

The results for one series of diaphragms, as shown in Figure 9, are discussed below. Diaphragms with stiffener depths greater than 190mm (11.5% of diaphragm height) all have approximately the same failure load. Failure is due to a local shear-compression buckle in the plate, with the stiffener remaining straight as shown in Figure 6. After buckling the plate is able to hang from the stiffeners in a tension field. This accounts for the post-buckling capacity.

For stiffener depths less than 100mm (5.5% of diaphragm depth) failure is due to overall buckling of the diaphragm, initiated by buckling of the stiffener. This is shown in Figure 5. These diaphragms have the post-buckling strength characteristic of slender unstiffened diaphragms.

There exists a diaphragm depth between 100mm and 190mm for which the elastic buckling loads of the stiffener and plate are equal. At this "critical" stiffener depth there are no alternate load paths in the diaphragm subsequent to buckling. For all of the series of diaphragms studied, the failure load was farthest below the elastic buckling load when the stiffener depth was close to this "critical" value.

When the diaphragm is loaded with an eccentric load, its capacity is significantly reduced, except in the case of diaphragms with heavy stiffeners. The failure mechanism also can change from a plate mechanism to an overall stiffened plate mechanism.

Analysis of all the diaphragms showed that when a diaphragm has a shear yield load significantly greater than the elastic buckling load, the failure load of the diaphragm is greater than the elastic buckling load. These diaphragms are relatively insensitive to the magnitude of plate geometric imperfections. When the shear yield load is close to the elastic buckling load, the failure load is significantly less than the elastic buckling load. These diaphragms are moderately sensitive to the magnitude of plate geometric imperfections. All the diaphragms are moderately sensitive to the magnitude of stiffener geometric imperfections.

4. DESIGN OF SUPPORT DIAPHRAGMS

There are several codes available which provide design rules for steel support diaphragms. All of them are based on load factor design, which in most instances represents a fore-runner to limit states design.

The code which first gave in-depth guidance to this problem was the Interim Design Rules, or the Merrison Report, which was published in England in 1973.[3] However due to the urgent need for this code at the time of its preparation, it was necessary to draft it as quickly as possible. As a result the rules became complex, and generally result in conservative designs. Subsequent work done at the Transport and Road Research Laboratory[4] resulted in proposed modifications that would make the rules less conservative.

North American design rules for box girders, including provisions for support diaphragms, have been proposed for inclusion into the AASHTO specifications.[5] Their physical incorporation is still (1981) pending.

This chapter will examine the different codes, and compare their design rules for support diaphragms. It is noted that the comparison should also extend to the loads to which the diaphragm can be subjected. Unfortunately, loads due to traffic, wind and temperature variation are difficult to compare between jurisdictions, due to differences in climate and legal truck configurations. For the purposes of this study, it will therefore be assumed that the design loads in the different codes represent actual loads, and do not include any built in factors of safety.

4.1 Interim Design Rules (Merrison Report)

These rules apply to diaphragms which are symmetrical, rectangular or trapezoidal (sides sloped less than 30° from the vertical) in shape and with a material yield stress less than 355MPa. This incorporates most of the common structural steels. The diaphragms are to be designed to resist vertical, horizontal, shear and out-of-plane stresses.

The bearing reaction force produces vertical forces in a support diaphragm. The designer may assume that these forces will be resisted by the diaphragm plate and its load-bearing stiffeners acting together, or by the load-bearing stiffeners only. The force distribution is approximated as going linearly from zero at the top to a maximum at the bottom. The maximum effective width of plate which can be assumed to act in concert with the stiffeners is shown in Figure 10. This width decreases towards the bottom of the diaphragm. Vertical stresses outside the effective width of plate used in the design are assumed to be redistributed into the effective width. When designing the plate, the stiffeners may not be taken as 100% effective in resisting load, and vice versa.

Horizontal stresses are due to deep beam action of the diaphragm across the bearing. The distribution of these stresses with diaphragm depth is non-linear, however, for design purposes it is assumed to be linear. Parts of the girder flanges, similar to those shown in Figure 8, are assumed to act together with the diaphragm. The horizontal stress distribution is modified by the effects of creep and shrinkage of the concrete deck, temperature differential between the concrete deck and

steel diaphragm, and by Poisson's effect of longitudinal stresses in the girder flanges. In addition, transverse shear stresses are taken to act on the cut edges of the girder flanges. Trapezoidal diaphragms are also subjected to horizontal stresses due to the horizontal component of shear in the girder webs. These stresses are assumed to be constant over the diaphragm depth.

Shear stresses are transferred into the diaphragm through the girder webs. Their actual distribution over the diaphragm depth is approximated by two straight lines, as shown in Figure 11. The equations of these lines are a function of the distance between the girder web and the edge of the bearing. Regions of the diaphragm subjected to low shear stresses, such as between load bearing stiffeners, are to be designed for 25% of the average shear stress at the girder web. This is a conservative simplification.

Additional vertical stresses are caused by horizontal forces acting perpendicularly to the plane of the diaphragm, and by eccentrically applied vertical forces. The horizontal forces are caused by traffic and wind loads, and by temperature variations. In addition, movements due to temperature variations may cause the diaphragm to be supported eccentrically on its bearing. It is also required that all diaphragms be designed for eccentricities beyond those caused by the applied loads and temperature variations, to account for construction tolerances when placing the bearing. The vertical stresses are assumed to increase linearly from zero at the top of the diaphragm to a maximum at the bottom, and must be resisted by full depth load-bearing stiffeners.

The Interim Design Rules are concerned only with the design of individual plate panels and stiffeners. It is assumed that if these components are adequately designed against instability, the overall stability of the diaphragm need not be a design consideration. This is due to the conservative assumptions that are made for the design of the plate panels and stiffeners, i.e. plate panels are simply supported and incapable of redistributing stress, and the plate has no stabilizing effect on the intermediate stiffeners.

In order to calculate the collapse load of an individual plate panel, its elastic buckling stress must first be determined. The actual state of stress at the boundaries of the panel is reduced to a set of normal and shear stresses, as shown in Figure 12. From these stresses and from the assumption of a simply supported plate, the elastic buckling stress can be determined.

The magnitude of the plate collapse stress is a function of the ratio of the elastic buckling stress to yield stress, geometry of the plate, state of stress at plate boundaries, and initial geometric imperfections. It can be determined from charts given in the Interim Design Rules, which in turn have taken the data from plate buckling studies. The plate collapse stress must be greater than the maximum equivalent stress in the panel, determined by combining the individual stresses in the panel using Von Mises criterion. In recognition of the fact that some yielding of the steel can occur prior to collapse, a boundary around the edge of the panel, with a width equal to 5 times the diaphragm thickness may be excluded when calculating the maximum equivalent stress.

Plate panels directly over the bearing and between the bearing and the girder web must be stocky enough so that redistribution of the stress concentrations at the bearing will not cause them to buckle.

Load-bearing stiffeners must be symmetrical about the mid-thickness of the diaphragm plate. Their maximum capacity is governed by either their yield stress or their torsional buckling stress, reduced by any residual stress effects.

The stresses applied to the stiffener include not only vertical stresses due to vertical and out-of-plane loads, but also stresses due to the P-Δ effect resulting from stiffener deformations. The assumed distribution of these stresses along the stiffener is shown in Figure 13. Their magnitude can be determined if the ratio of stiffener elastic buckling load to applied load, the stiffener slenderness ratio, and the initial geometric imperfections are known. The elastic buckling load must take into account both stabilizing and destabilizing effects from the adjoining plate. The stabilizing effects are a function of the geometry of the diaphragm only, whereas the destabilizing effects are a function of geometry as well as horizontal stresses in the plate. The effective slenderness ratio of the stiffener decreases with increasing eccentricity of the applied load.

Intermediate stiffeners divide the diaphragm into individual panels. Their design is based on criteria similar to those used for load-bearing stiffeners. However, the design equations for intermediate stiffeners are based on having a minimum slenderness ratio, rather than a minimum load capacity. Intermediate stiffeners may be placed on one side of the diaphragm only. As a result of this

unsymmetrical shape, the stiffener will have collapse loads that depend on the buckling direction. The diaphragm plate is assumed to have no stabilizing effect on the stiffeners. This is conservative, but specific data is very scarce.

4.2 TRRL Modifications to Interim Design Rules

Modifications to the Interim Design Rules have been proposed by the Transport and Road Research Laboratory, based on the results of a large deflection inelastic finite element program. A study of these results has given a simpler failure criterion, which can be applied to diaphragms with load bearing stiffeners only. Basically, failure of the plate has occurred when it reaches yield at the center of the shear-and-compression buckle in the lower half of the outer panel, as shown in Figure 14. This allows for some yielding of the plate around the bearing and along the web prior to collapse. The loads corresponding to this first yield criterion are approximately 75 to 90% of the collapse loads.

The failure criterion for the stiffener is first yield. This can occur at loads from 92% of the collapse load (concentric loading) to 65% of the collapse load (loading with 10mm eccentricity). For larger eccentricities this failure criterion may be even more conservative.

To determine the collapse load of the plate, the stresses at Point C (see Figure 14) must first be determined. The vertical stresses are calculated on the assumption that a constant effective width of the plate acts together with the load-bearing stiffeners.

Finite element analyses have shown that decreasing the effective width at the bottom of the diaphragm, as is required by the Interim Design Rules, produces overly conservative designs. Horizontal stresses are calculated in the same manner as for the Interim Design Rules, with the exception that no shear stresses are applied to the cut edges of the girder flanges. The horizontal stress at Point C is taken to be one-sixth the horizontal stress calculated at the bottom flange. Both the vertical and horizontal stresses calculated in this manner are conservative, compared to the results of finite element analysis.

The shear stress at Point C (see Figure 14) is taken as the average shear stress in the plate. This is unconservative, because the actual shear stress distribution is nonuniform with local stresses exceeding the average by 20%. However, it is felt to be justified because of the conservative assumptions made when determining the vertical and horizontal stresses.

Based on these computations, the elastic buckling stress is determined using the procedure given in the Interim Design Rules. With the elastic buckling stress and geometric imperfections of the plate known, the state of stress which will cause yielding i.e. failure at Point C, can be determined.

The failure loads obtained for the plate by these methods are conservative, compared to the finite element results. However, they are 5 to 20% less conservative than those found by using the Interim Design Rules.

The load-bearing stiffener capacities are checked, using a procedure similar to the one of the Interim Design Rules. However,

several discrepancies in the Interim Design Rules have been corrected. First, the stiffener elastic buckling loads were found to be greater than those given by the finite element results. It appeared that the stabilizing influence of the plate on the stiffener had been included twice. Thus, an effective width of plate had been assumed to act together with the stiffener when calculating stiffener properties. The same width of plate was incorporated an additional time by using a plate stabilizing term in calculating the stiffener elastic buckling load. This was corrected by taking the stiffener buckling load to be the buckling load of the stiffener acting alone, plus a portion of the unstiffened plate buckling load. The portion of unstiffened plate buckling load depends on the ratio of stiffener buckling load to plate buckling load, and automatically provides a destabilizing effect if the plate buckles before the stiffener.

The second discrepancy concerns the effective width of plate to be used when calculating vertical stresses in the stiffener. The narrowing of the effective width at the bottom of the diaphragm is overly conservative, as finite element results show no peak in the vertical stresses at this point. The stress distributions applied to the stiffener are otherwise the same as those used in the Interim Design Rules.

With the applied stresses, the elastic buckling load and the initial geometric imperfections known, the load on the stiffener which causes first yield can be calculated.

Although the discrepancies in the Interim Design Rules appear to be self-cancelling under concentric loading, this is not true when

eccentric loads are applied. The modified rules are 10% less conservative for a loading eccentricity of 10mm. In addition, they correctly predict the location of first yield in the stiffener, whereas the Interim Design Rules do not.

4.3 Proposed Design Specifications for AASHTO

These design specifications have been heavily influenced by the Interim Design Rules. In fact, the Interim Design Rules are given as a general reference for the clauses relating to diaphragms.

Vertical forces in the diaphragm are due to the bearing reaction force. They are assumed to vary linearly from zero at the top of the diaphragm to a maximum at the bottom. The effective width of plate which can be assumed to act together with the load-bearing stiffeners in resisting vertical forces is not given. However, a maximum effective width of 18 times the diaphragm thickness is implied, as this is the effective width of plate to be used when calculating stiffener sectional properties. The effective width can not be greater than the width of the bearing, plus 2 times the flange thickness at the base of the diaphragm.

Horizontal stresses in the diaphragm are due to deep beam action of the diaphragm spanning over the bearing, and the horizontal component of shear in sloping girder webs. They are calculated using the same assumptions as the Interim Design Rules. The only exceptions are that the transverse shear stresses on the outside faces of the girder flanges may be taken as zero, and that Poisson's effect of the longitudinal stresses in the girder flanges is neglected.

Shear stresses in the diaphragms are due to transfer of shear from the webs to the bearing. They are assumed to be uniformly distributed over the diaphragm depth although lower panels in stiffened diaphragms are to be designed for stability using a 30% increase in shear stress. This is in recognition of the fact that large local stresses may occur in the lower regions of the diaphragm. To keep these stresses to a minimum, the girder web is not to be closer to the bearing than 0.2 times the diaphragm depth.

Vertical stresses due to horizontal loads acting perpendicularly to the diaphragm, and due to eccentrically applied vertical loads must be resisted by full depth load-bearing stiffeners. All diaphragms must be designed for an eccentricity in addition to that caused by the applied loads. This will account for construction tolerances in placing the bearing.

Design rules are given to ensure that the individual plate panels have adequate strength and stability. In addition, the panels in the lower portion of the diaphragm are to be stocky (depth to thickness ratio less than 40), to allow for some redistribution of stress. As in the Interim Design Rules, the overall stability of the diaphragm need not be a design consideration if its individual components are adequately designed against collapse. This is probably conservative although the evidence is not conclusive.

The stability of the plate panels is checked, assuming that they are subjected to horizontal compression and shear stresses only. The panel is assumed to be capable of redistributing any vertical stresses to the load-bearing stiffeners, including their effective width of plate.

The individual capacities of the panel in shear, compression and bending are determined seperately. For stocky panels the plate capacity is governed by yielding, while for slender panels it is governed by elastic buckling. A transition curve between these two cases (which is a function of the ratio of elastic buckling load to yield load) is provided for panels which fail due to inelastic buckling. The transition curve takes into account the weakening effects of residual stresses and geometric imperfections on the plate.

The panel design stresses are taken as those midway between the panel edges, as shown in Figure 15. Unlike the Interim Design Rules, which consider stresses at each point individually when determining plate capacity, these rules consider stresses in a region. This is a more realistic concept, as collapse of the panel is a function of the stress distribution throughout the panel rather than the stress at a single point. If more than one type of stress is present, an interaction equation based on elastic theory is used to determine overall plate capacity.

The applied shear stresses can not exceed the shear yield stress, modified for the simultaneous prescence of axial stresses. In addition, the equivalent stress at any point in the panel as determined by the Von Mises criterion can not exceed the yield stress.

Load-bearing stiffeners are designed as compression members, and must be symmetric about the diaphragm mid-thickness line. An effective width of plate is assumed to act together with them, but no other stabilizing or destabilizing effects of the plate are considered. However, design rules are given to ensure that the ratio of the moment

of inertia of the stiffener to that of the adjacent plate is large enough to keep any destabilizing forces to a minimum. The applied stresses are assumed to vary linearly from zero at the top of the stiffener to a maximum at the bottom.

The stiffeners are designed for strength and stability, using the provisions presently in AASHTO for the design of columns subjected to axial load and moment. These are the same provisions as those used for the design of load-bearing stiffeners in plate girders. In addition, the maximum bearing stress at the base of the stiffeners can not exceed the yield stress. A restriction is also placed on the maximum slenderness of a load-bearing stiffener, in order to keep the torsional buckling stress higher than the yield stress.

Intermediate stiffeners divide the diaphragm into panels, and may be located on one side of the diaphragm only. Intermediate vertical stiffeners are designed to satisfy the rigidity and torsional buckling requirements for load-bearing stiffeners. Intermediate horizontal stiffeners include an effective width of diaphragm plate, and are to be designed as columns. The design load is the horizontal compression stress acting at the stiffener location, multiplied by the effective stiffener area. This load is applied eccentrically, to account for any initial geometric imperfections. In addition, the horizontal stiffener must have sufficient rigidity to force the development of a nodal line in the buckled diaphragm. The requirements preventing torsional buckling of vertical stiffeners also apply to horizontal stiffeners.

4.4 Comparison of Design Rules

A typical support diaphragm was designed according to the three design specifications described in this chapter, and details of this design are given in the Appendix. AASHTO specified loads were used when designing to all three specifications, but were increased differently by using the load factors required by each specification. The applied loads correspond to a girder span of approximately sixty meters.

The maximum slenderness provisions for plate panels in the lower regions of the diaphragm were not enforced for any of the specifications, as the Transport and Road Research Laboratory specification has no such restriction. This allowed the diaphragms to be designed according to the three different specifications for direct comparison. In an actual design, the diaphragm plate would either have to be thickened, or a horizontal stiffener added, to limit the slenderness ratio.

Figure 16 shows the diaphragms designed according to the three different specifications. The only dimension which varies, according to which specification is used, is the stiffener depth. It decreases by 33% when the Interim Design Rules are modified using the Transport and Road Research Laboratory proposals. This is to be expected as one of the major objectives of the Transport and Road Research Laboratory proposals is to make the Interim Design Rules less conservative for stiffeners under eccentric loading. The stiffener depth for the diaphragm designed according to the proposed AASHTO specifications is midway between the other two depths. Small differences in required diaphragm dimensions do not show up in this comparison as the plate

thicknesses used must be those which are commercially available. It should be noted that the load factors used in the proposed AASHTO specifications are the load factors presently used by AASHTO. Lower load factors may be justified, as the weakening effects of geometric imperfections and residual stresses which are traditionally accounted for in the load factors have already been accounted for in the proposed specifications.

The proposed AASHTO design specifications will be used for designing the diaphragms in Chapter 5 of this report for the following reasons:

1. Although they have the disadvantage of being in the proposal stage at this time, in their basic form it is likely that they will be the standard for design of diaphragms in North America.

2. They are the most recent design rules and therefore reflect the most up-to-date thinking on the subject.

3. They contain the simplest provisions of all that have been evaluated here. The design of each component is not radically affected by the design of the other components.

5. EFFICIENCY OF SUPPORT DIAPHRAGM SYSTEMS

This chapter will examine three different diaphragm systems for their efficiency in carrying load from the girder webs to the bearing. The systems examined are unstiffened diaphragms, diaphragms with load-bearing stiffeners only, and diaphragms with load-bearing stiffeners and a single horizontal stiffener. Out-of-plane stresses are not considered in this comparison. These stresses are totally resisted by the load-bearing stiffeners, and have no influence on the design of the diaphragm plate. The diaphragm thicknesses considered in this comparison range from 8 to 24mm.

Figure 17 shows a plot of diaphragm capacity versus diaphragm thickness for unstiffened diaphragms. The shear yield capacity is the maximum capacity the diaphragm can attain, even with stiffeners added.

The yield capacity of the diaphragm is the load at which the maximum equivalent stress (according to the Von Mises criterion) in the plate equals the yield stress. Widening the bearing under an unstiffened diaphragm can substantially increase the yield capacity, as the vertical stress is the dominant stress.

The buckling capacity of the plate governs the capacity of the diaphragm. For the 24mm thick diaphragm, the buckling capacity is less than 14% of the shear yield capacity, and this ratio decreases for smaller diaphragm thicknesses.

The addition of load-bearing stiffeners to the diaphragm separates the plate into two halves. This increases the buckling capacity of the plate significantly, as shown in Figure 18. It is interesting to note

that for all but the extreme diaphragm thicknesses, plate failure is due to inelastic buckling. Residual stresses and geometric imperfections therefore have a decidedly weakening effect, as expected. For thicknesses greater than approximately 24mm, the buckling strength of the plate exceeds the shear yield capacity, and any additional stiffeners will not increase the strength.

Figure 18 also shows the yield capacity of the diaphragm when infinitely large stiffeners are used, i.e. the vertical stresses go to zero. In practise there would be an economical limit to the maximum size of stiffener, and the yield capacity of the diaphragm would be lower than that shown.

In order for the diaphragm to satisfy the maximum plate slenderness requirements, a horizontal stiffener must be added. Figure 19 shows the buckling capacities for the upper as well as the lower plate panels for this case. For plate thicknesses greater than approximately 12mm, the buckling capacity of the lower plate panel is governed by shear yielding. The corresponding line in Figure 19 plots below the overall shear yield capacity line of the diaphragm, because the lower plate panel is designed for a shear stress which is 30% greater than the average shear stress. The buckling capacity of the upper plate panel exceeds that of the lower plate panel. The capacity of diaphragms more than 12mm thick therefore will not be increased by the addition of more stiffeners. Lower plate panels less than 12mm thick are not permitted by the design specifications, as their slenderness ratio exceeds that required for a proper stress redistribution.

Load-bearing stiffeners are sized such that the yield capacity

of the diaphragm plate will not govern the design. The size of the lighter stiffeners is governed by stiffener capacity, rather than by the yield strength of the plate.

Of the three diaphragm systems considered, only the diaphragm with a horizontal stiffener satisfies the proposed AASHTO design specifications. The stiffener should be located at a distance of 35 to 40 times the plate thickness above the bottom flange. This will ensure that the lower plate panel fails in shear yielding, while keeping the upper plate panel dimensions to a minimum.

The thickness of the diaphragm plate will be governed by the required capacity of either the upper plate panel or the lower plate panel. If the height of the diaphragm is greater than approximately 170 times its thickness, the upper plate panel capacity will govern the design. Otherwise, the lower plate panel capacity will govern. The most efficient design results when both plate panels have the same capacity, i.e. when the diaphragm plate has a slenderness ratio of approximately 170. If the applied loads on the diaphragm require that a different plate thickness be used, then the efficiency of the diaphragm will decrease.

Once the plate thickness has been selected, the load-bearing stiffeners can be designed. They must be sufficiently heavy to prevent the maximum equivalent stress in the diaphragm from exceeding the yield stress.

6. SUMMARY AND CONCLUSIONS

This study has examined the behavior of steel support diaphragms in box girder bridges and the design specifications that may be used for their design.

Tests on typical diaphragms have shown that failure is due to inelastic buckling. This may be an overall buckling mode of the diaphragm, including stiffeners or it may be a local buckling failure of the plate outside the bearing. Geometric imperfections, and to a lesser extent residual stresses, reduce the failure capacity of the diaphragm.

Diaphragms are subjected to a complex state of stress which includes vertical, horizontal, and shear in-plane stresses, as well as out-of-plane bending stresses. The distribution of these stresses can not be adequately described by simple analytical methods.

Large deflection, inelastic finite element programs have been used to analyse steel support diaphragms. They give an adequate description of the actual diaphragm behavior if the diaphragm boundary conditions are known. These programs have been used to conduct parametric studies on diaphragms with load-bearing stiffeners only. These studies give relationships between shear yield load, elastic buckling load, and collapse load for different diaphragms with different geometric imperfections.

Three different design specifications were examined for use in designing diaphragms. They were the Interim Design Rules,[3] the Transport and Road Research Laboratory modifications[4] to the Interim

Design Rules, and the proposed specification for AASHTO[5]. The proposed AASHTO design specification was chosen as the most satisfactory set of rules for designing diaphragms. Although it has not yet been formally approved as such, it reflects some of the latest thinking on the subject of diaphragm design. Also, it is the simplest to apply of any of the available design specifications.

A design study of diaphragm systems was performed, using the proposed AASHTO specifications. It was found that the most efficient diaphragm has load-bearing stiffeners and one horizontal stiffener, located approximately 40 times the diaphragm plate thickness above the bottom flange. The study also showed that the closer the diaphragm height is to approximately 170 times the diaphragm thickness, the more efficient the diaphragm will be.

REFERENCES

1. Dowling, P. J., "Strength of Steel Box Girder Bridges", ASCE, Vol. 101, ST9, Sept. 1975, pp. 1929-1946.
2. "Steel Box Girder Bridges - Ultimate Strength Considerations", by the Subcommittee on Ultimate Strength of Box Girders of the ASCE-AASHTO Committee on Flexual Members, ASCE, Vol. 100, ST12, Dec. 1975, pp. 2433-2448.
3. "Inquiry into the Basis of Design and Method of Erection of Steel Box Girder Bridges," (Merrison Report), London, 1973.
4. Crisfield, M.A. and Puthli, R. S., "A Design Approach for Lightly Stiffened Box Girder Diaphragms", Transport and Road Research Lab, Supplementary Report 393, 1978.
5. Wolchuk and Mayrbaurl, "Proposed Design Specifications for Steel Box Girder Bridges", Report No. FHWA-TS-80-205, 1980.
6. Dowling, P. J., Loe, J. A. and Dean, J. A., "The Behavior up to Collapse of Load Bearing Diaphragms in Rectangular and Trapezoidal Stiffened Steel Box Girders", Paper #7, Proceedings of the International Conference on Steel Box Girder Birdges, The Institute of Civil Engineers, London, 1973, pp. 95-117, 169-170.
7. Irwin, C. A. K. and Loe, J. A., "Loading Tests on the Stiffened Diaphragms of a Trapezoidal Steel Box Girder", Transport and Road Research Lab, Lab Report 824, 1978.
8. Crisfield, M. A., "Theoretical and Experimental Behavior of Lightly Stiffened Box-Girder Diaphragms", Transport and Road Research Lab, Lab Report 961, 1980.

9. Puthli, R. S. and Crisfield, M. A., "The Strength of Stiffened Box Girder Diaphragms", Transport and Road Research Lab, Supplementary Report 353, 1977.

10. Crisfield, M. and Puthli, R., "A Finite Element Method Applied to the Collapse Analysis of Stiffened Box Girder Diaphragms", Paper #13, Proceedings of the International Conference on Steel Plated Structures, London, 1976, pp. 311-337.

11. Puthli, R. S., Supple, W. J. and Crisfield, M. A., "Collapse Behavior of Rectangular Steel Box Girders", The Structural Engineer, Dec. 1978, pp. 75-80, 84.

8. FIGURES

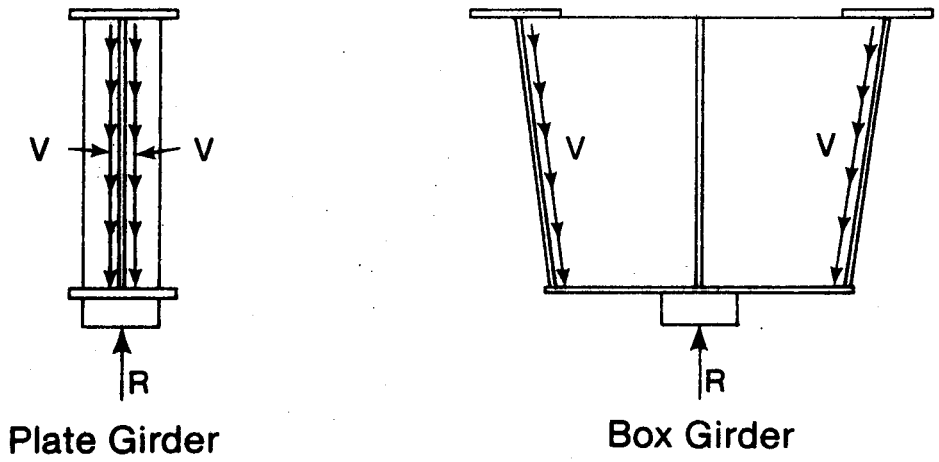

Figure 1 - Transfer of Vertical Load from Girder Webs to Bearings: Comparison of Plate Girder and Box Girder Behavior

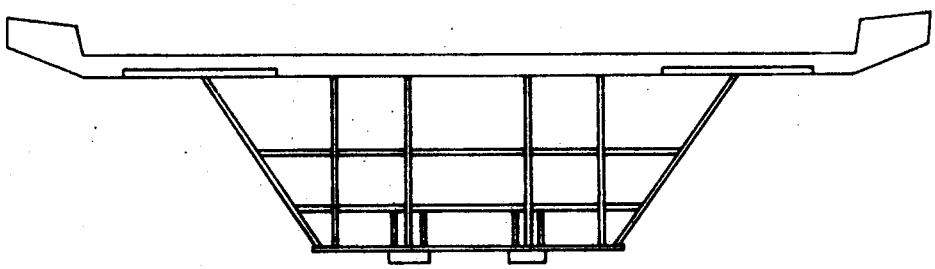

(a)

Typical Long Span Cross Section

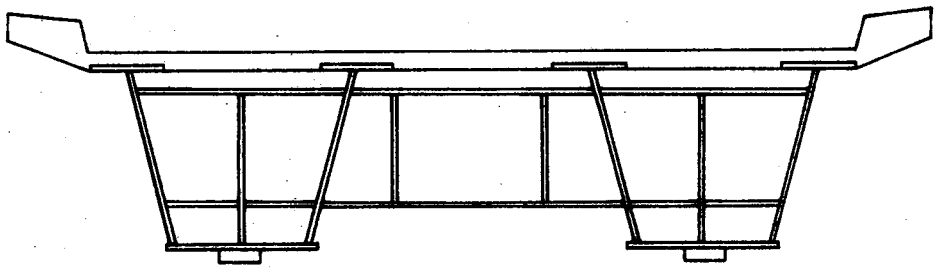

(b)

Typical Medium to Short Span Cross Section

Figure 2 - Steel Box Girder Bridges

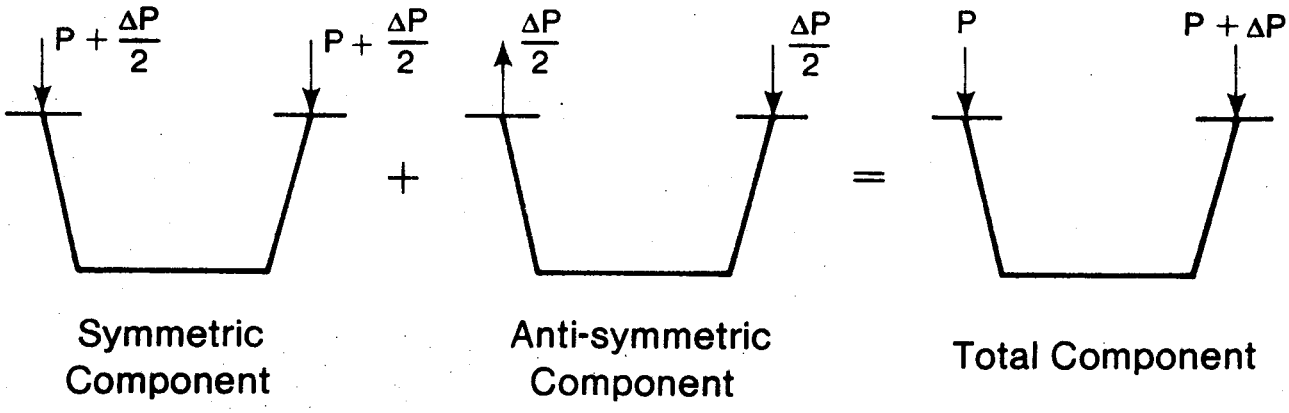

Figure 3 - Components of Vertical Load to be Transferred by Support Diaphragms

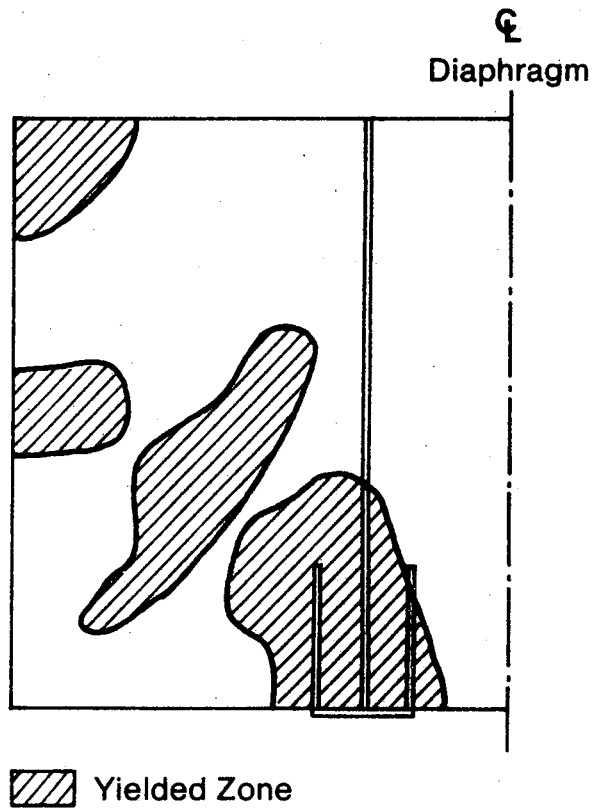

Figure 4 - Yield Zone in Support Diaphragm at 86% of Capacity (from Ref. 8)

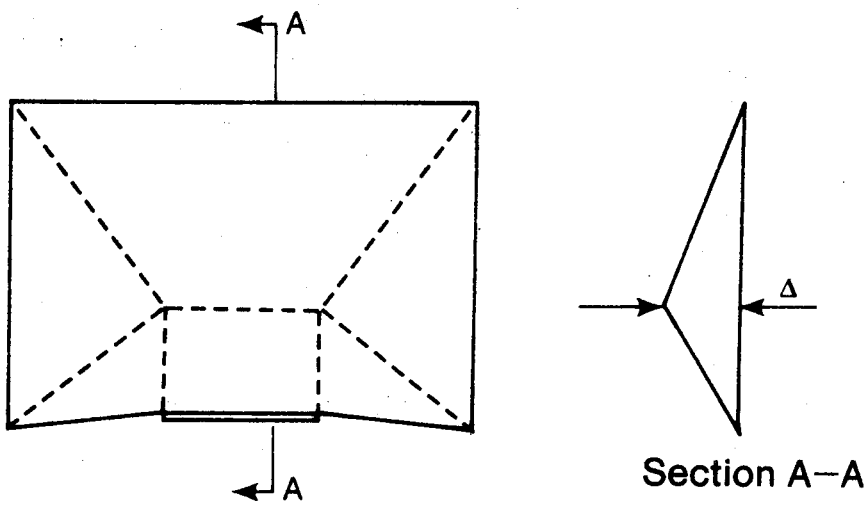

Figure 5 - Failure Mechanism for Unstiffened Diaphragm

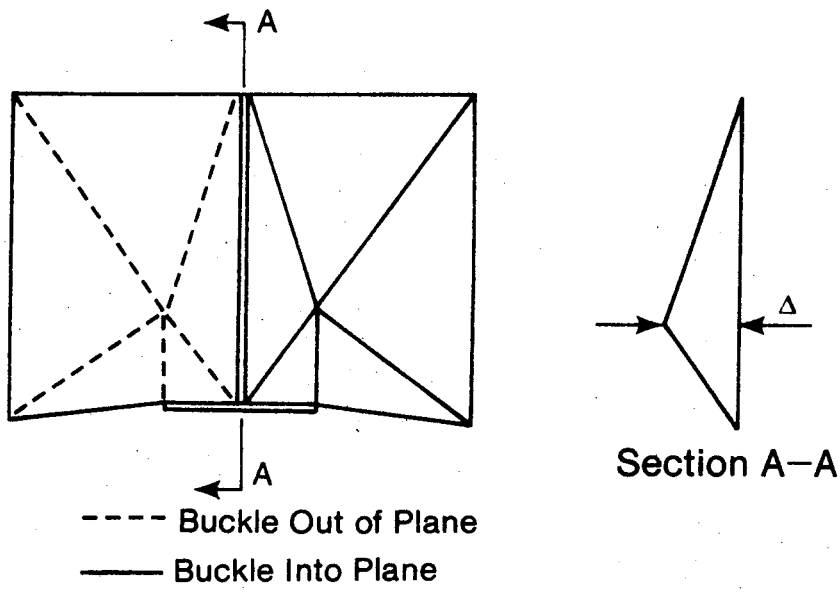

Figure 6 - Plate Failure Mechanism for Stiffened Diaphragm

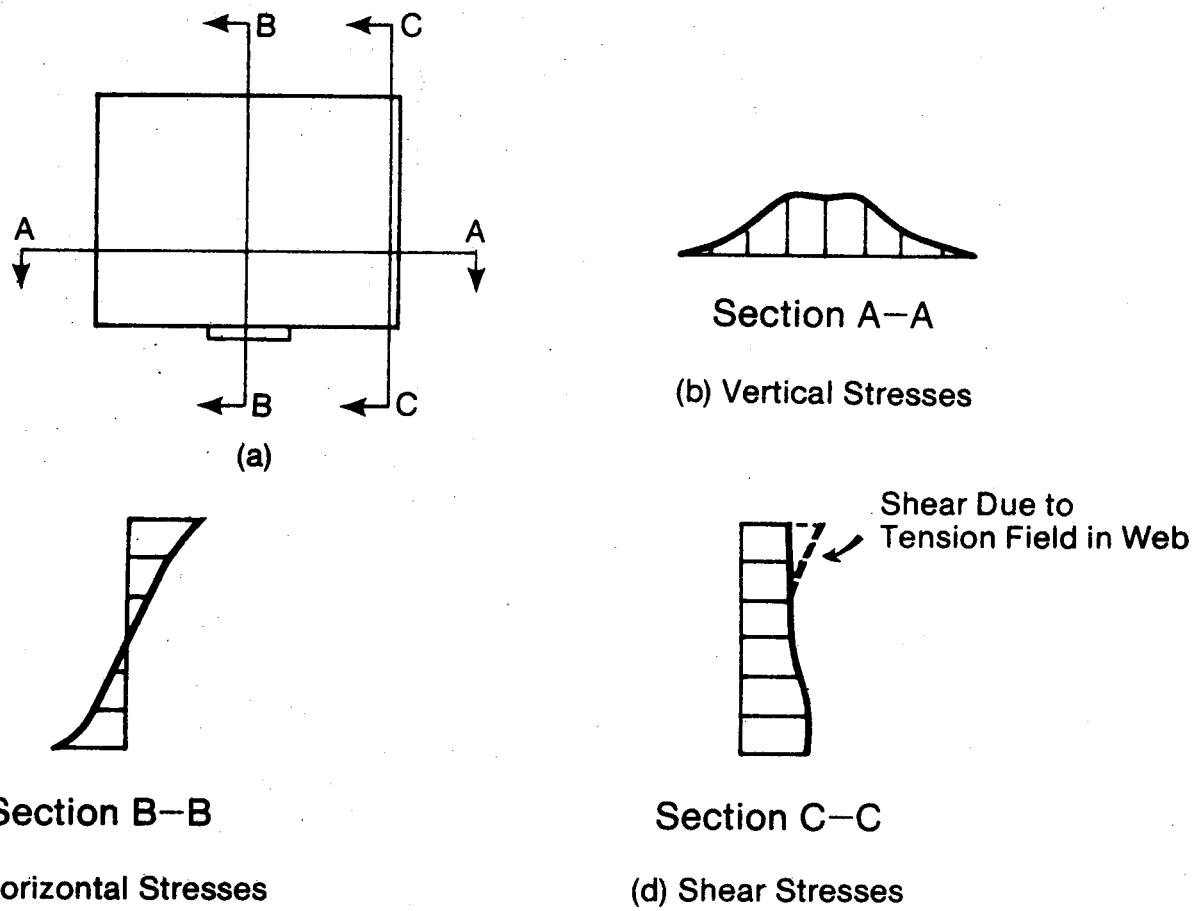

Figure 7 - Stress Distributions in Support Diaphragms

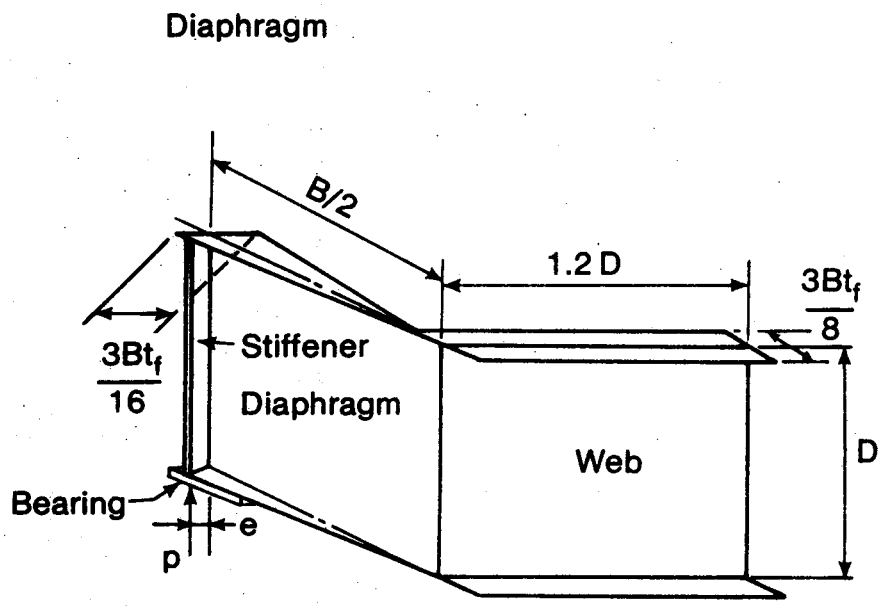

t_d = Diaphragm Thickness
t_w = Web Thickness = 1.2 t_d
t_f = Flange Thickness = 2.5 t_d

Figure 8 - Structural Model of Diaphragm, Web and Flanges

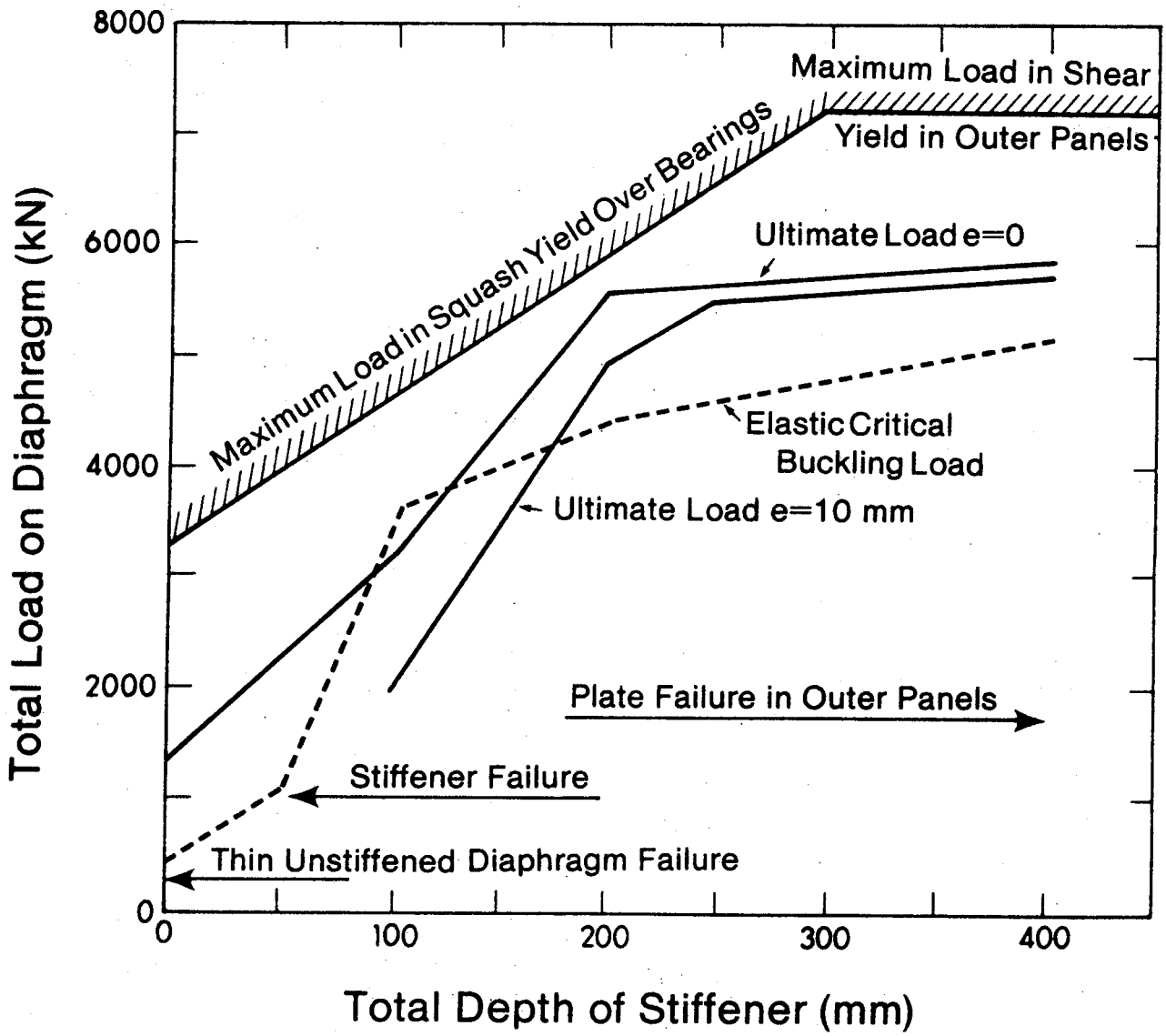

Figure 9 - Relationships Between Load and Depth of Stiffener (from Ref. 9)

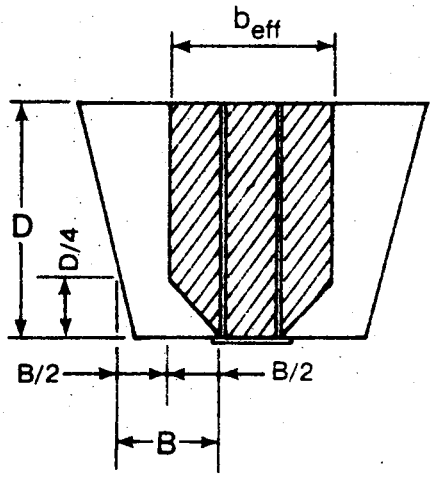

Figure 10 - Effective Width of Diaphragm Plate

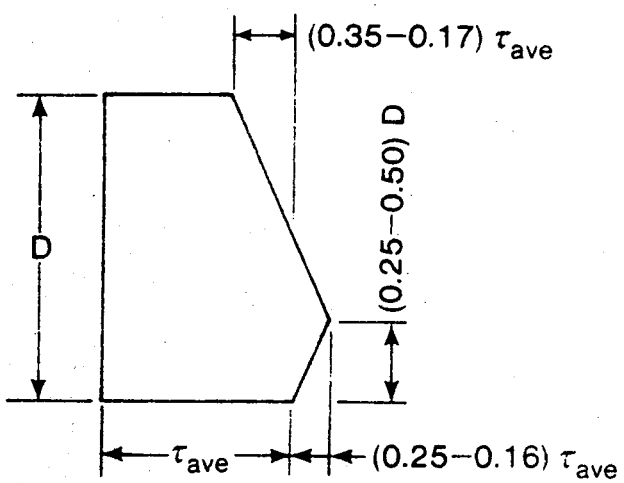

Figure 11 - Shear Stress Distribution for Usual Diaphragm Proportions

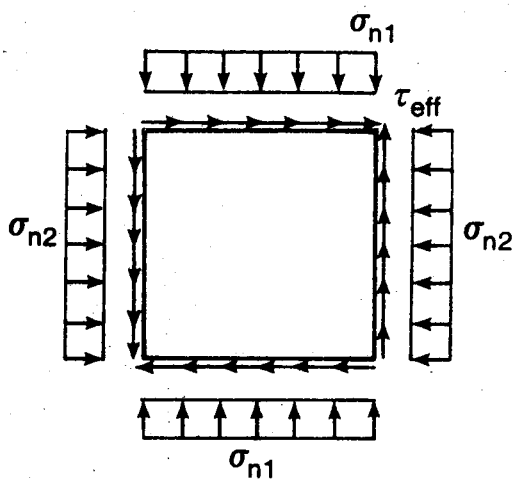

Figure 12 - Equivalent Stresses for Determining Elastic Buckling Stress

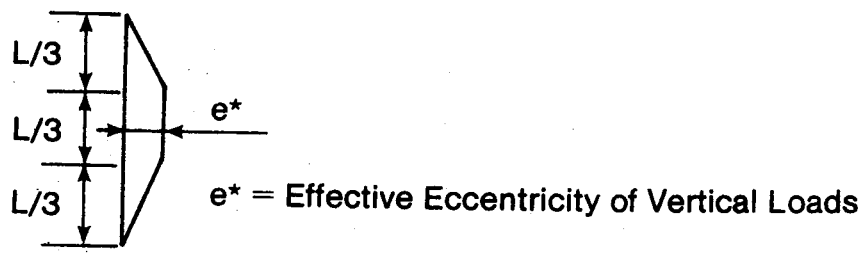

Figure 13 - Distribution of Additional Stresses due to Stiffener Deformations

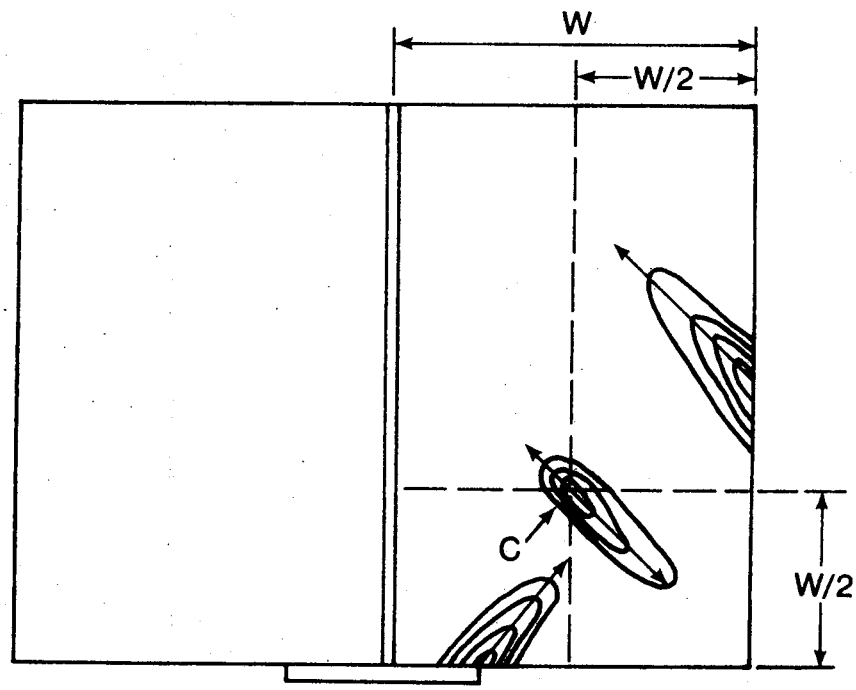

Figure 14 - Growth of Yield Zones in Diaphragm Plate

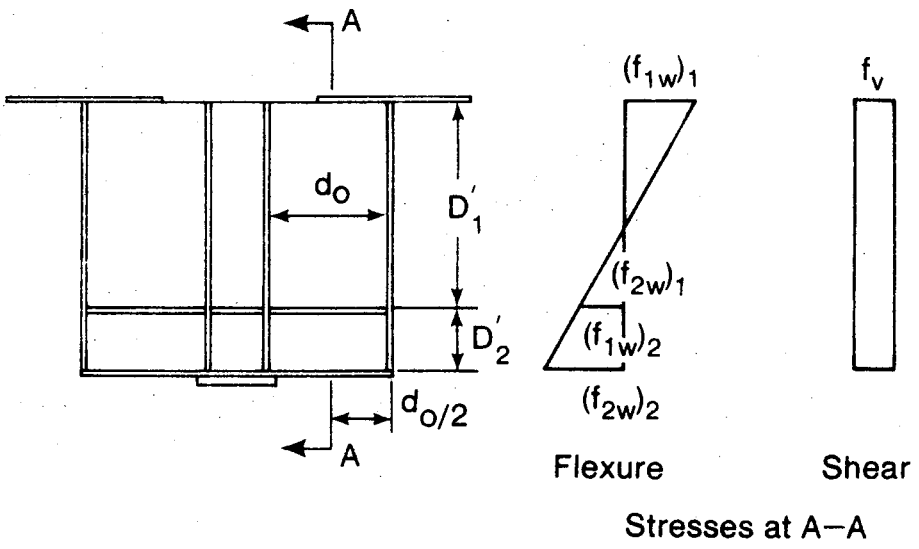

Figure 15 - Design Stresses for Plate Panels

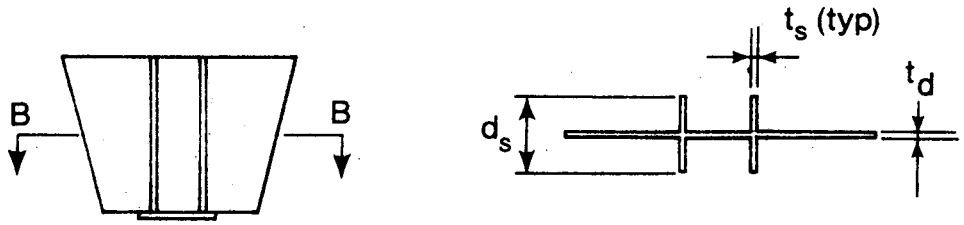

Specification	t_d (mm)	d_s (mm)	t_s (mm)
Interim Design Rules	18	600	30
Transport and Road Research Lab.	18	400	30
Proposed AASHTO Rules	18	500	30

Figure 16 - Design Dimensions of Steel Support Diaphragms

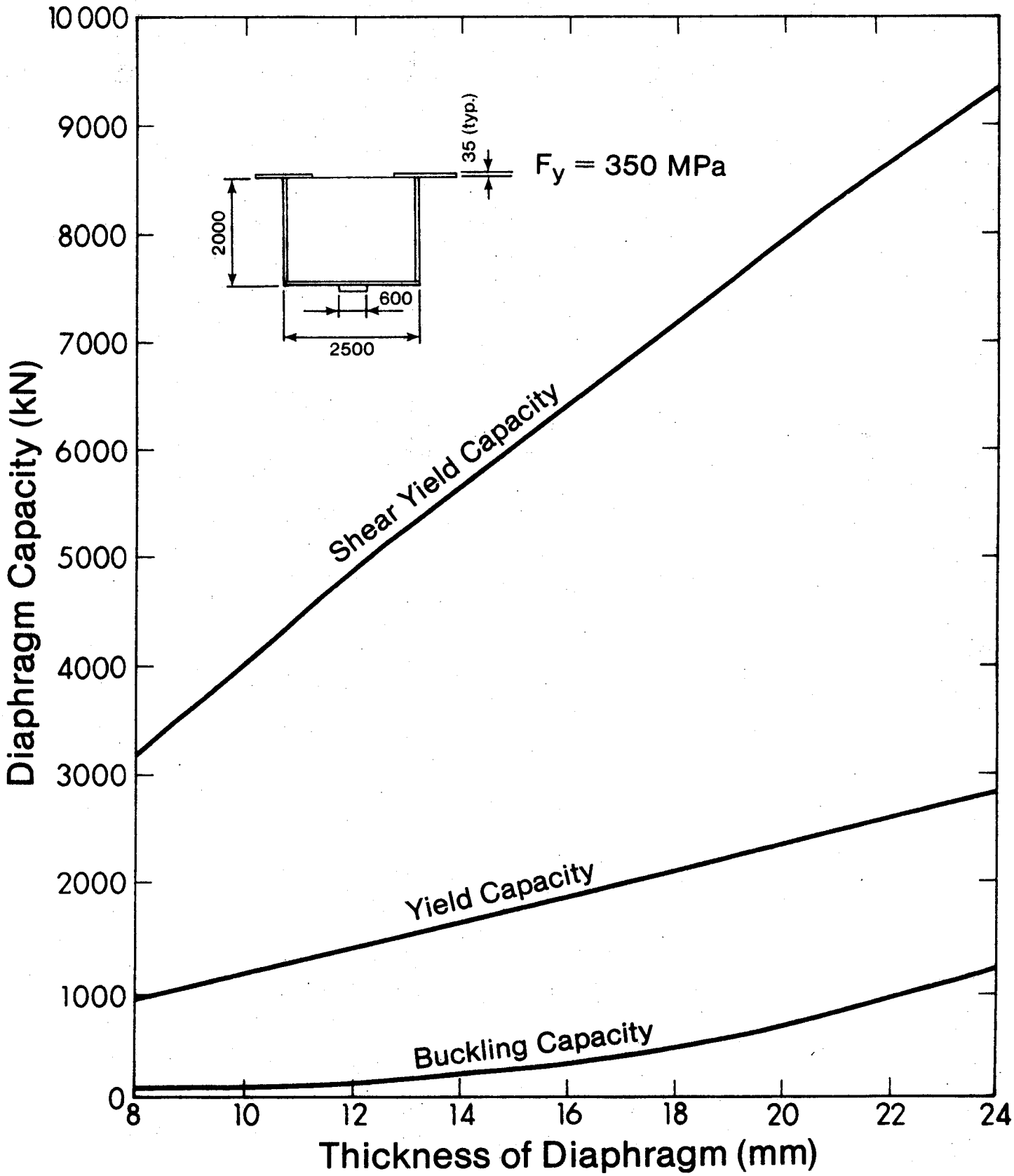

Figure 17 - Capacity of Unstiffened Support Diaphragms

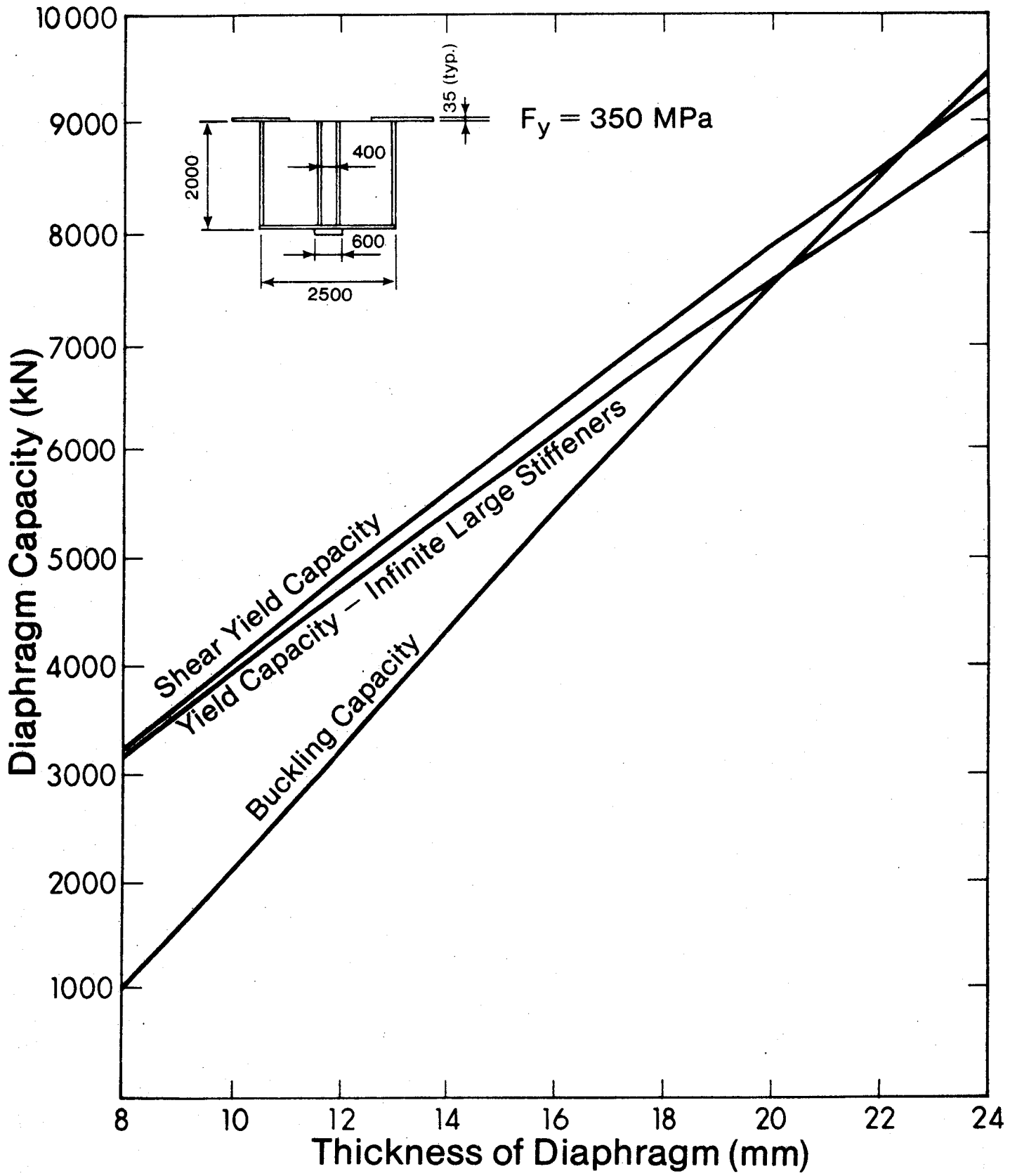

Figure 18 - Capacity of Support Diaphragm with Load-Bearing Stiffeners

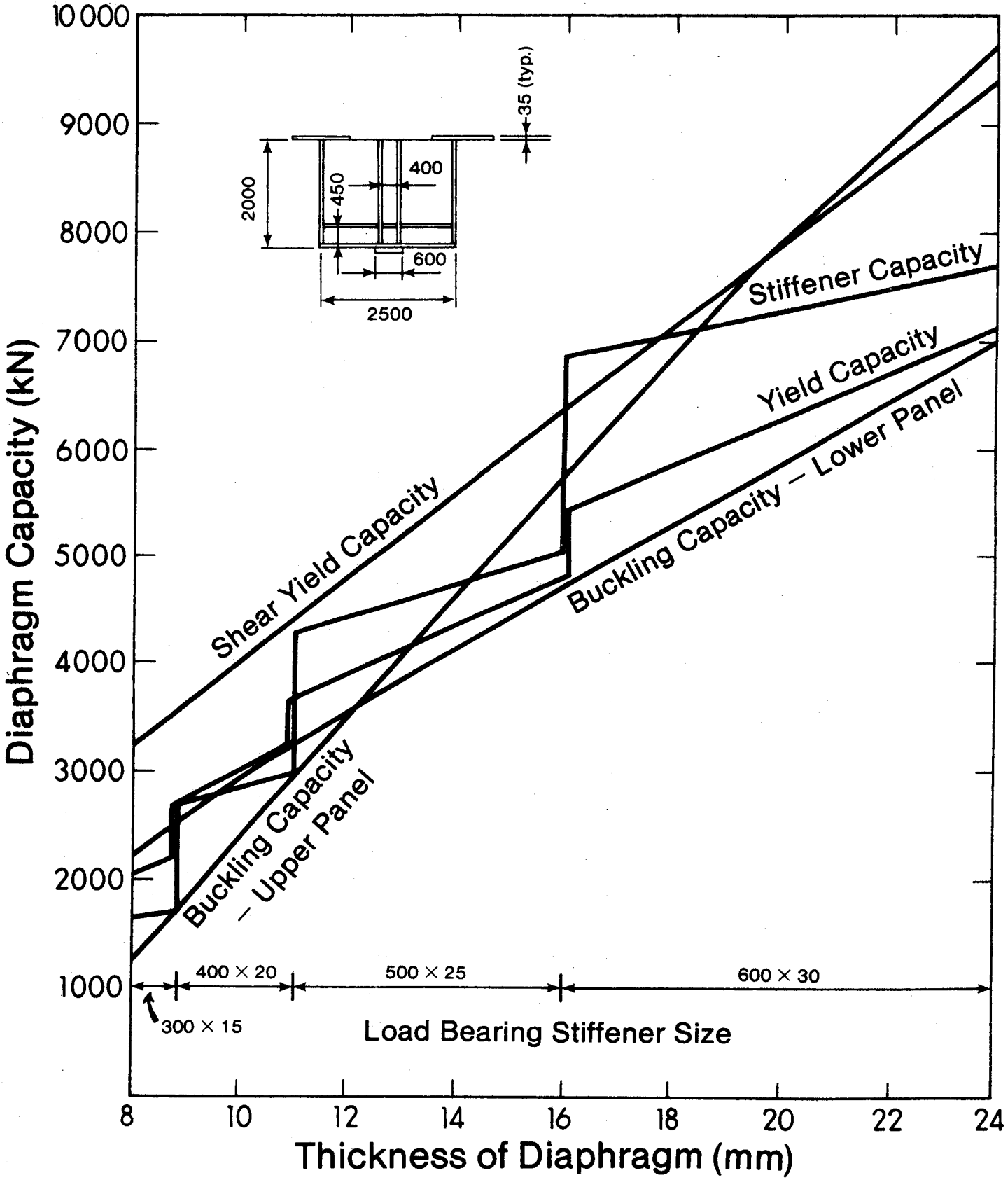

Figure 19 - Capacity of Support Diaphragm with Load-Bearing and One Horizontal Stiffener

APPENDIX:

SAMPLE DESIGN OF STEEL SUPPORT DIAPHRAGMS

DESIGN OF STEEL SUPPORT DIAPHRAGMS

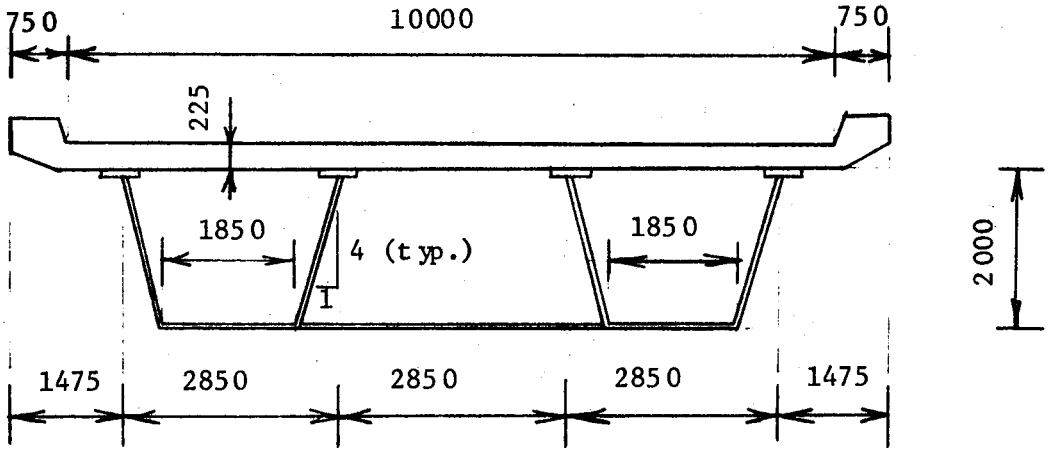

F_y = 350 MPa

Flanges - top 800 mm x 40 mm

- bottom 1850 mm x 35 mm

Bearings - 600 mm x 600 mm (rocker bearings)

Vertical loads

- dead load - 1000 kN/web (concrete deck)
  - 350 kN/web (steel box)
  - 250 kN/web (wearing surface)
- live load - 850 kN/web

Horizontal load perpendicular to diaphragm

- temperature - 250 kN acting at centroid of box

A. DESIGN BY INTERIM DESIGN RULES (MERRISON REPORT)

Try 18 mm plate with twin 600 mm x 30 mm load-bearing stiffeners (ignore maximum plate slenderness provisions - Clause 11.3.1)

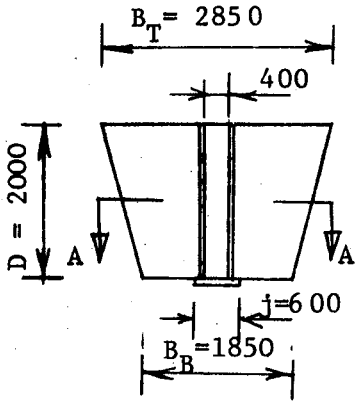

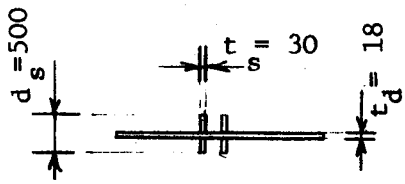

Design plate panel between load-bearing stiffener and web

Position of reference equivalent stress - Clause 11.2.6:

by inspection, $5t_d$ = 90 mm above the bottom flange and $5t_d$ = 90 mm inside the load bearing stiffener

Vertical stress - Clause 11.2.2:

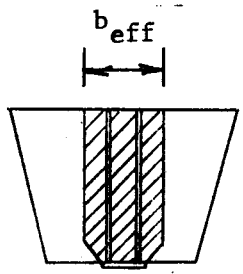

At distance 485 mm above bottom flange:

$$b_{eff} = \frac{B_B - j}{2} + \frac{B_T - B_B}{8} + j = \frac{1850-600}{2} + \frac{2850-1850}{8} + 600 = 1350 \text{ mm}$$

At position of reference equivalent stress:

$$b_{eff} = j + 2 \cdot 90 \text{ mm} = 600 + 2 \cdot 90 = 780 \text{ mm}$$

Vertical load on diaphragm - Clause 4.2:

Combination 'a'

$R_v = 2[(1.1 \cdot 350) + (1.2 \cdot 1000) + (1.25 \cdot 250) + (1.5 \cdot 850)] = 6345$ kN ← governs

Combination 'b'

$R_v = 2[(1.1 \cdot 350) + (1.2 \cdot 1000) + (1.25 \cdot 250) + (1.25 \cdot 850)] = 5920$ kN

ΣA_{sz} - area of stiffeners

$= (600-18) \cdot 30 \cdot 2 = 34920$ mm^2

$$\sigma_1 = \frac{R_v(1-z/D)}{0.75\Sigma A_{sz} + b_{eff} \cdot t_D}$$ z - height above bottom flange

At distance 485 mm above bottom flange:

$$\sigma_1 = \frac{6345000\ (1-485/2000)}{(0.75 \cdot 34920)+(1350 \cdot 18)} = 95 \text{ MPa}$$

At position of reference equivalent stress:

$$\sigma_1 = \frac{6345000\ (1-90/2000)}{(0.75 \cdot 34920)+(780 \cdot 18)} = 151 \text{ MPa}$$

Horizontal stress - Clause 11.2.4:

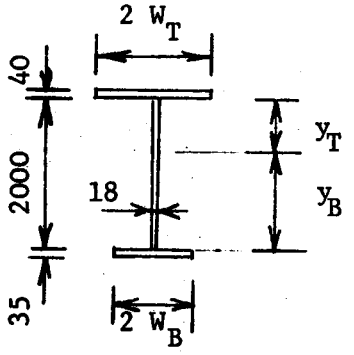

Effective section resisting horizontal stresses

At distance 485 mm outside load-bearing stiffener:

$$W_T = \left[\left(\frac{B_T-400}{2}\right)-485\right] \cdot \frac{1}{4} = \left[\left(\frac{2850-400}{2}\right)-485\right] \cdot \frac{1}{4} = 185 \text{ mm} \quad 2W_T = 370 \text{ mm}$$

$$W_B = \left[\left(\frac{B_B-400}{2}\right)-485\right] \cdot \frac{1}{4} = \left[\left(\frac{1850-400}{2}\right)-485\right] \cdot \frac{1}{4} = 60 \text{ mm} \quad 2W_B = 120 \text{ mm}$$

$Y_B = 1195$ mm $\quad Y_T = 805$ mm $\quad I = 2962000$ cm^4 $\quad \Sigma A = 55000$ mm^2

At position of reference equivalent stress:

$$W_T = \left[\left(\frac{2850-400}{2}\right) - 90\right] \cdot \frac{1}{4} = 285 \text{ mm} \qquad 2W_T = 570 \text{ mm}$$

$$W_B = \left[\left(\frac{1850-400}{2}\right) - 90\right] \cdot \frac{1}{4} = 160 \text{ mm} \qquad 2W_B = 320 \text{ mm}$$

$Y_B = 1170$ mm $\qquad Y_T = 830$ mm $\qquad I = 4531000$ cm^4 $\qquad \Sigma A = 70000$ mm^2

Applied moment:

$$M = \frac{R_v}{2} \cdot S + \frac{R_v}{2}\left(\frac{B_T - B_B}{2D}\right)(Y_B - D/2)$$ - conservative to ignore other effects i.e. transverse shears, Poissons effect, etc.

S - lever arm of vertical load

At distance 485 mm outside load bearing stiffener:

$$S = \left(\frac{B_T + B_B}{4}\right) - 485 - 200 = \left(\frac{2850+1850}{4}\right) - 485 - 200 = 490 \text{ mm}$$

$$M = \frac{6345}{2} \cdot 0.49 + \frac{6345}{2}\left(\frac{2850-1850}{2 \cdot 2000}\right)\left(1.195 - \frac{2.00}{2}\right) = 1710 \text{ kN-m}$$

$$\sigma_{b2} = \frac{1710000}{2962000} \cdot (-80.5) = -46 \text{ MPa at top of diaphragm}$$

$$\sigma_{b2} = \frac{1710000}{2962000} \cdot (119.5) = 69 \text{ MPa at bottom of diaphragm}$$

$$\sigma_2 = \frac{R_v}{2\Sigma A}\left(\frac{B_T - D_B}{2D}\right) = \frac{6345000}{2 \cdot 55000} \cdot \left(\frac{2850-1850}{2 \cdot 2000}\right) = 14 \text{ MPa}$$

At position of reference equivalent stress:

$$S = \left(\frac{2850+1850}{4}\right) - 90 - 200 = 885 \text{ mm}$$

$$M = \frac{6345}{2} \cdot 0.885 + \frac{6345}{2}\left(\frac{2850-1850}{2 \cdot 2000}\right)\left(1.17 - \frac{2.00}{2}\right) = 2940 \text{ kN-m}$$

$$\sigma_{b2} = \frac{2940000}{4531000} \cdot 108 = 70 \text{ MPa at reference point}$$

$$\sigma_2 = \frac{6345000}{2 \cdot 70000} \cdot \left(\frac{2850-1850}{2 \cdot 2000}\right) = 11 \text{ MPa}$$

Shear stress - Clause 11.2.5:

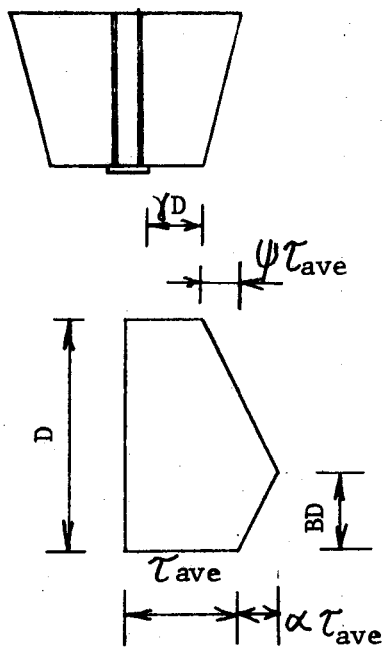

$$\gamma = \left(\frac{1850-600}{2\cdot2000}\right) = 0.31$$

from Fig. 11.7

$\alpha = 0.18$

$\psi = 0.25$

$\beta = 0.36$

shear stress

$$\tau ave = \frac{R_v}{2D\cdot t_D} = \frac{6345000}{2\cdot2000\cdot18} = 88 \text{ MPa}$$

At position of reference equivalent stress:

$$\tau = 88 + (0.18\cdot88)\frac{90}{0.36\cdot2000} = 90 \text{ MPa}$$

Reference equivalent stress

$$\sigma_e = \sqrt{\sigma_1^2+\sigma_2^2-\sigma_1\cdot\sigma_2+3\tau^2} = \sqrt{151^2+81^2-151\cdot81+3\cdot90^2} = 204 \text{ MPa}$$

Calculate capacity of panel - Clause 11.3.2.1:

treat panel as equivalent rectangular panel, height-2000 mm, width-975 mm

Equivalent stresses at panel boundaries

Vertical stress:

take at section $\frac{975}{2} \cong 485$ mm above bottom flange

using Fig. 11.8

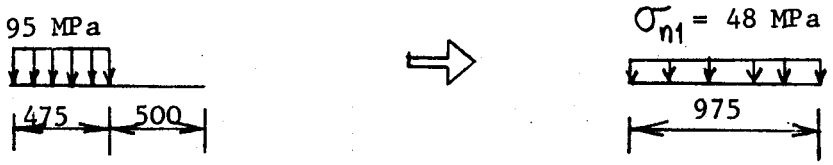

Horizontal stress:

take at section $\frac{975}{2} \cong 485$ mm outside load-bearing stiffener

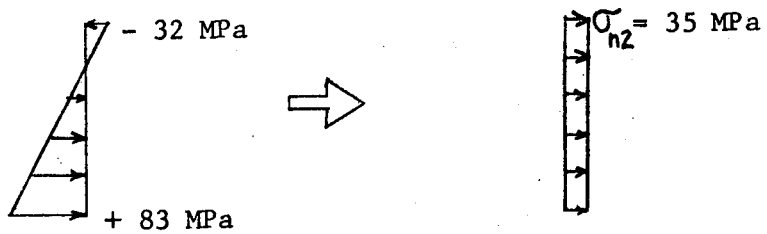

$$\sigma_{n2} = \frac{83-32}{2} + \frac{83+32}{12} = 35 \text{ MPa}$$

Shear stress:

$$\tau_{eff} = \tau_{ave} = 88 \text{ MPa}$$

$$\sigma_e = \sqrt{48^2+35^2-48 \cdot 35+3 \cdot 88^2} = 158 \text{ MPa}$$

$$\phi = \frac{\text{panel height}}{\text{panel width}} = \frac{2000}{975} = 2.05$$

$$\frac{\sigma_{n1}}{\sigma_{n2}} = \frac{48}{35} = 1.37 \qquad \frac{\sigma_{n1}}{\sigma_e} = \frac{48}{158} = 0.30 \qquad \frac{\sigma_{n2}}{\sigma_e} = \frac{35}{158} = 0.22$$

Elastic buckling stress:

$$\sigma_{e_{crit}} = k' \cdot \frac{\pi^2 E}{11} \left(\frac{t_d}{975} \right)^2$$

from Fig. 11.10 $k' = 4.6$

$$\sigma_{e_{crit}} = 4.6 \frac{\pi^2 \cdot 200000}{11} \left(\frac{18}{975}\right)^2 = 281 \text{ MPa}$$

$$\frac{\sigma_{e_{crit}}}{\sigma_y} = \frac{281}{350} = 0.80$$

Collapse stress:

from Fig. 11.11 $\frac{\sigma_{e_{ult}}}{\sigma_y} = 0.73$ $\sigma_{e_{ult}} = 0.73 \cdot 350 = 256$ MPa

$\frac{256}{1.2}$ MPa = 213 MPa

required capacity = 204 MPa therefore OK

Design plate panel between load bearing stiffeners

Position of reference equivalent stress - Clause 11.2.6

By inspection: $5t_d$ = 90 mm above bottom flange and midway between the load-bearing stiffeners

Vertical stress - Clause 11.2.2:

at distance 200 mm above bottom flange

$b_{eff} = j + 2 \cdot 200 = 600 + 2 \cdot 200 = 1000$ mm

$$\sigma_1 = \frac{6345000\ (1-200/2000)}{(0.75 \cdot 34920)+(1000\ 18)} = 129 \text{ MPa}$$

At position of reference equivalent stress

σ_1 = 151 MPa as for first panel

Horizontal stress - Clause 11.2.4:

Midway between stiffeners

$W_T = \frac{2850}{8} = 355$ mm $2W_T = 710$ mm

$W_B = \frac{1850}{8} = 230$ mm $2W_B = 460$ mm

Y_B=1155 mm Y_T=845 mm I=5625000 cm^4 ΣA=80500 mm^2

$$S = \left(\frac{B_T+B_B}{4}\right) - \frac{j}{4} = \left(\frac{2850+1850}{4}\right) - \frac{600}{4} = 1025 \text{ mm}$$

$$M = \frac{6345}{2} \cdot 1.025 + \frac{6345}{2}\left(\frac{2850-1850}{2\cdot2000}\right)\left(1.155-\frac{2.00}{2}\right) = 3375 \text{ kN-m}$$

$$\sigma_{b2} = \frac{3375000}{5625000} \cdot -84.5 = -51 \text{ MPa} \quad \text{at top of diaphragm}$$

$$\sigma_{b2} = \frac{3375000}{5625000} \cdot 115.5 = 69 \text{ MPa} \quad \text{at bottom of diaphragm}$$

$$\sigma_{b2} = \frac{3375000}{5625000} \cdot 106.5 = 64 \text{ MPa} \quad \text{at reference equivalent stress}$$

$$\sigma_2 = \frac{6345000}{2\cdot80500}\left(\frac{2850-1850}{2\cdot2000}\right) = 10 \text{ MPa}$$

Shear stress - Clause 11.2.5:

$$\tau = \frac{R_v}{8D\cdot t_D} = \frac{6345000}{8\cdot2000\cdot18} = 22 \text{ MPa}$$

Reference equivalent stress

$$\sigma_e = \sqrt{151^2+64^2-151\cdot64+3\cdot22^2} = 137 \text{ MPa}$$

Calculate capacity of panel - Clause 11.3.2.1:

height = 2000 mm width = 400 mm

$$\phi = \frac{2000}{400} = 5.0$$

Equivalent stresses at panel boundaries

Vertical stress:

take at section $\frac{400}{2}$ = 200 mm above bottom flange

σ_{n1} = 129 MPa

Horizontal stress:

take midway between load-bearing stiffeners

$$\sigma_{n2} = \frac{79-41}{2} + \frac{79+41}{12} = 29 \text{ MPa}$$

Shear stress:

τ_{eff} = 22 MPa

$\sigma_e = \sqrt{129^2+29^2-129\cdot29+3\cdot22^2}$ = 123 MPa, use 129 MPa

Elastic buckling stress:

$\frac{\sigma_{n1}}{\sigma_{n2}} = \frac{129}{29} = 4.45$ $\frac{\sigma_{n1}}{\sigma_e} = \frac{129}{129} = 1.0$ $\frac{\sigma_{n2}}{\sigma_e} = \frac{29}{129} = 0.22$

from Fig. 11.10 k'=3.0

$\sigma_{e_{crit}} = 3.0\cdot\frac{\pi^2\cdot200000}{11}\cdot\left(\frac{18}{400}\right)^2 = 1090$ MPa

$\frac{\sigma_{e_{crit}}}{\sigma_y} = \frac{1090}{350} = 3.11$

Collapse stress:

from Fig. 11.11 $\frac{e_{ult}}{\sigma_y} = 0.80$ $\sigma_{e_{ult}} = 0.80\cdot350=280$ MPa

$\frac{280}{1.2} = 233$ MPa

required capacity = 137 MPa therefore OK

Design load-bearing stiffeners

Vertical stress - Clause 11.2.2:

At base of stiffener:

b'_{eff} = 600 mm R_v = 5920 kN comb 'b'

$\sigma_{ls} = \frac{R_v}{0.65b'_{eff}t_D+\Sigma A_{sz}} = \frac{5920000}{0.65\cdot600\cdot18+34920} = 141$ MPa

At 667 mm above bottom flange:

b'_{eff} = 1350 mm

$\sigma_{ls} = \frac{5920000(1-667/2000)}{0.65\cdot1350\cdot18+34920} = 78$ MPa

Out-of-plane bending stresses - Clause 11.2.3:

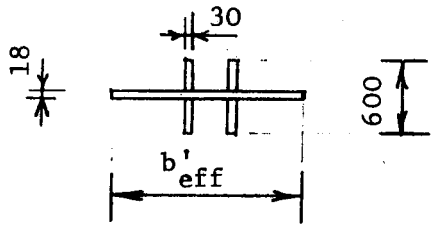

e_n = 10 mm - Clause 4.7.1

R_h = 1.2•250 = 300 kN

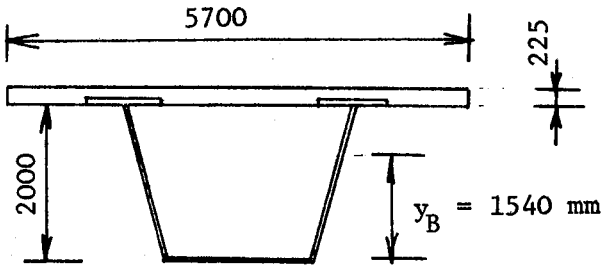

$$e = 10 + \frac{300 \cdot 1540}{5920} = 88 \text{ mm}$$

At base of stiffener:

$$\sigma_{bn} = \frac{R_v \cdot e}{\Sigma I_x} \left(d_s + \frac{t_D}{2}\right) \qquad \Sigma I_x = 108026 \text{ cm}^4$$

$$= \frac{5920 \cdot 88}{108026} \cdot 25 = 121 \text{ MPa}$$

$$[\sigma_{ls}] = 141 + 121 = 262 \text{ MPa}$$

At 667 mm above bottom flange:

$$\Sigma I_x = 108063 \text{ cm}^4$$

$$\sigma_{bn} = \frac{5920 \cdot 88}{108063} \cdot 25 \left(1 - \frac{667}{2000}\right) = 80 \text{ MPa}$$

$$[\sigma_{ls}] = 78 + 80 = 158 \text{ MPa}$$

Design of load-bearing stiffener - Clause 11.4.1

Minimum thickness of stiffener:

$$t_s > \frac{\sqrt{jds}}{16} = \frac{\sqrt{600 \cdot (300-18/2)}}{16} = 26 \text{ mm therefore OK}$$

Torsional buckling stress - Clause 10.3.1:

$$\frac{t_s}{t_d}\left(\frac{d_s}{b}\right)^3$$ b - distance between stiffener and web

$$= \frac{30}{18}\left(\frac{281}{975}\right)^3 = 0.04 \qquad \frac{b}{t_s} = \frac{975}{30} = 32.5$$

from Fig. 10.7 $\sigma_{YT_1} = 90$ MPa

$$\sigma_{YT2} = 50\frac{(10t_s)^3}{A_s d_s} \qquad A_s = 281 \cdot 30 = 8430 \text{ mm}^2$$

$$= 50\frac{(10 \cdot 30)^3}{8430 \cdot 281} = 5700 \text{ MPa}$$

therefore $\sigma_{YT2} > \sigma_Y$

Residual stresses - Chapter 7:

take $\sigma_{R_1} = 30$ MPa - see Fig. 7.3(e)

$$\sigma'_{YS} = \sigma_Y - \sigma_{R_1} = 350-30 = 320 \text{ MPa}$$

At base of stiffener:

$$\sigma_{1s_{char}} = \frac{320}{1.2} = 267 \text{ MPa}$$

$[\sigma_{1s}] = 262$ MPa therefore OK

Horizontal stresses in plate at stiffener:

$$W_T = \left(\frac{2850-400}{2}\right)\frac{1}{4} = 305 \text{ mm} \qquad 2W_T = 610 \text{ mm}$$

$$W_B = \left(\frac{1850-400}{2}\right)\frac{1}{4} = 180 \text{ mm} \qquad 2W_B = 360 \text{ mm}$$

$$Y_B = 1165 \text{ mm} \qquad Y_T = 835 \text{ mm} \qquad I = 4844000 \text{ cm}^4 \qquad \Sigma A = 73000 \text{ mm}^2$$

$$S = \left(\frac{2850+1850}{4}\right) - 200 = 975 \text{ mm}$$

$$M = \frac{5920}{2} \cdot 0.975 + \frac{5920}{2}\left(\frac{2850-1850}{2 \times 2000}\right)\left(1.165-\frac{2.00}{2}\right) = 3010 \text{ kN-m}$$

$$\sigma_{b2} = \frac{3010000}{4844000} \cdot -83.5 = -52 \text{ MPa} \quad \text{at top of diaphragm}$$

$$\sigma_{b2} = \frac{3010000}{4844000} \cdot 116.5 = 73 \text{ MPa} \quad \text{at bottom of diaphragm}$$

$$\sigma_2 = \frac{5920000}{2 \cdot 73000}\left(\frac{2850-1850}{2 \cdot 2000}\right) = 10 \text{ MPa}$$

$$[\sigma_{2s}] = 10 + \left(\frac{73-56}{2}\right) + \left(\frac{73+56}{12}\right) = 29 \text{ MPa}$$

$$\left[\frac{L}{d_o}\right]_{eff} = \frac{L}{d_o}\left[\frac{1}{1+55\left(\frac{D_e R_v}{EI_x}\right)}\right]$$

$$= \frac{2000}{300}\left[\frac{1}{1+55\left(\frac{2000 \cdot 88 \cdot 5920000}{200000 \cdot 1080630000}\right)}\right] = 5.26$$

$$\lambda_c = \frac{\frac{n^2 EI_x}{L^2} + b'_{eff} t_d q_1 + \frac{0.35 EL^2 t_D{}^3}{b'_{eff} \cdot b_s{}^2}\left(1 + \frac{5bs}{L}\right)}{0.5R_v + \frac{0.4L^2 t_d}{b'_{eff}}\,[\sigma_{2s}]}$$

$$b_s = \left(\frac{B_T+B_B}{2}\right) = \left(\frac{2850+1850}{2}\right) = 2350 \text{ mm}$$

$$q_1 = 1.96E\left(\frac{t_D}{b_s}\right)^2 = 1.96 \cdot 200000 \cdot \left(\frac{18}{2350}\right)^2 = 23.0 \text{ MPa}$$

$$\lambda_c = \frac{\frac{\pi^2 \cdot 200000 \cdot 1080630000}{2000^2} + 1350 \cdot 18 \cdot 23 + \frac{0.35 \cdot 200000 \cdot 2000^2 \cdot 18^3}{1350 \cdot 2350}\left(1+5.\frac{2350}{2000}\right)}{0.5 \cdot 5920000 + \frac{0.4 \cdot 2000^2 \cdot 18 \cdot 29}{1350}}$$

= 150

from Fig. 11.21 $\sigma_a \simeq 20$ MPa

At 667 mm above bottom flange:

$$\sigma_{ls_{char}} = \frac{320-20}{1.2} = 250 \text{ MPa}$$

$[\sigma_{ls}] = 158$ MPa therefore OK

B. DESIGN USING TRRL MODIFICATIONS TO INTERIM DESIGN RULES

try 18 mm plate with 400 x 30 stiffeners

Plate check

Vertical stress:

Effective width of plate:

$b_{eff} = 1350$ mm

$R_v = 6345$ kN

$\Sigma A_{sz} = (400-18) \cdot 30 \cdot 2 = 22920 \text{ mm}^2$

At distance 485 mm above bottom flange:

$$\sigma_1 = \frac{6345000\ (1-485/2000)}{(0.75 \cdot 22920)+(1350 \cdot 18)} = 176 \text{ MPa}$$

Horizontal stress:

At distance 485 mm outside load-bearing stiffener:

$\sigma_{b2} = 69$ MPa at bottom of diaphragm (from design by Interim Design Rules)

$\sigma_2 = 14$ MPa

Shear stress:

$$\tau_{ave} = \frac{6345000}{2000 \cdot 18 \cdot 2} = 88 \text{ MPa}$$

Stresses at Point C:

$\sigma_x^* = 116$ MPa

$\sigma_y^* = \frac{69}{6} + 14 = 26$ MPa

$\tau^* = 88$ MPa

$\sigma_e = \sqrt{116^2+26^2-116\cdot26+3\cdot88^2} = 185$ MPa

$\phi = \frac{2000}{975} = 2.05$

$\frac{\sigma_{n1}}{\sigma_{n2}} = \frac{116}{26} = 4.46$ $\quad \frac{\sigma_{n1}}{\sigma_e} = \frac{116}{185} = 0.63$ $\quad \frac{\sigma_{n2}}{\sigma_e} = \frac{26}{185} = 0.14$

from Fig. 11.10, Interim Design Rules

$k' = 4.5$

$\sigma_{e_{crit}} = 4.5 \frac{\pi^2\cdot200000}{11} \cdot \left(\frac{18}{975}\right)^2 = 276$ MPa

$\frac{\sigma_e}{\sigma_{e_{crit}}} = \frac{185}{276} = 0.67$

for initial imperfection of 3.0 mm

$\frac{\Sigma\delta}{t_d} = \frac{3.0}{18} = 0.17$

from Fig. 19.19 - Part III, Interim Design Rules

$\frac{\Sigma\sigma}{\sigma_{e_{crit}}} = 1.21$ $\qquad \Sigma\sigma = 1.21\cdot276 = 334$ MPa

$$\sigma_{e_{peak}} = \sqrt{\sigma_e^2+n(\Sigma\sigma-\sigma_e)[n(\Sigma\sigma-\sigma_e)+2\sigma_1-\sigma_2]} \qquad n = 1$$

$$= \sqrt{185^2+1(334-185)[1(334-185)+2\cdot116-26]}$$

$$= 295 \text{ MPa}$$

allowable stress $= \frac{350}{1.2} = 292$ MPa 1% over therefore OK

Stiffener check

Critical buckling load of outer plate panel:

$$P_{P1} = \frac{\sigma_{e\,crit}}{\sigma_e} \cdot \frac{R_v}{2} = \frac{276}{185} \cdot \frac{6345}{2} = 4735 \text{ kN}$$

Critical buckling load of unstiffened plate:

Clause 11.3.2.2 - Interim Design Rules

$$k_1 = 3.4 + \frac{2.2D}{B_B} = 3.4 + \frac{2.2 \cdot 2000}{1850} = 5.78$$

$$k_2 = 0.4 + \frac{j}{2B_B} = 0.4 + \frac{600}{2 \cdot 1850} = 0.56$$

$$k_3 = 1 - \frac{14°}{100} = 0.86$$

$$k_4 = 1.0$$

$$k = 5.78 \cdot 0.56 \cdot 0.86 \cdot 1.0 = 2.78$$

$$P_{ust} = 0.5 \frac{kEt_d^3}{D} = 0.5 \frac{2.78 \cdot 200000 \cdot 18^3}{2000} = 811 \text{ kN}$$

Critical buckling load of stiffener:

$$P_{st} = 1.981 \frac{n^2 EI}{D^2} = 1.981 \cdot \pi^2 \cdot \frac{200000 \cdot 30400^3}{2000^2 \cdot 12} = 156400 \text{ kN}$$

Combined buckling load:

$$P_c = P_{st} + P_{ust}\left(1 - \frac{P_{st}}{P_{P1}}\right) = 156400 + 811\left(1 - \frac{156400}{5210}\right) = 132860 \text{ kN}$$

$$A_1 P^2 - A_2 P + A_3 = 0$$

$$A_1 = \frac{x}{DA_t}\left(1 + \frac{ed_s}{2r^2}\right) - \frac{4.0 \cdot e \cdot k}{\pi}$$

$$A_2 = \sigma_y + \frac{P_c x}{DA_t}\left(1 + \frac{ed_s}{2r^2}\right) + q_o k P_c$$

$$A_3 = P_c \sigma_y$$

$$k = \frac{xd_s}{2DA_t r^2}\left(\sin\pi\frac{x}{D} - .069\sin 2\pi\frac{x}{D}\right) + \frac{d_s}{2\pi A_t r^2}\left(\cos\pi\frac{x}{D} + 2\frac{x}{D} - 1 - \frac{.069}{2}\cos 2\pi\frac{x}{D} + \frac{.069}{2}\right)$$

$$A_t = \frac{1350 \cdot 18}{2} + 382 \cdot 30 = 23610 \text{ mm}^2$$

$$I = \frac{400^3 \cdot 30}{12} + \frac{1350}{2 \cdot 12} \cdot 18^3 = 160328050 \text{ mm}^4$$

$$r^2 = \frac{160328050}{23610} = 6790 \text{ mm}^2$$

$e = 88$ mm - from design by Interim Design Rules

$q_o = 2.5$ mm - assumed geometric intersection

by trial and error, critical section is at bottom flange $x = D$

$k = 0$

$$A_1 = \frac{1}{23610}\left(1 + \frac{88 \cdot 400}{2 \cdot 6790}\right) = .000152$$

$$A_2 = .350 + \frac{132860}{23610}\left(1 + \frac{88 \cdot 400}{2 \cdot 6790}\right) = 20.56$$

$$A_3 = 132860 \cdot .35 = 46500$$

$P = 4600$ kN

$$P_{all} = \frac{4600}{1.2} = 3830 \text{ kN}$$ applied load = 2960 kN therefore OK

C. DESIGN BY PROPOSED AASHTO SPECIFICATIONS

try 18 mm plate with 600 x 30 stiffeners

Design of Panel

Horizontal stress - Clause 1.7.215(C)(3):

At section 485 mm outside load-bearing stiffener:

from design by interim design rules

$f_{1w} = -32$ MPa at top of diaphragm

$f_{2w} = 83$ MPa at bottom of diaphragm

vertical load = 1.3(1000+350+250+1.67·850) = 3925 kN

therefore

$$f_{1w} = -32\,\frac{3925}{6345/2} = -40 \text{ MPa}$$

$$f_{2w} = 83\,\frac{3925}{6345/2} = 103 \text{ MPa}$$

Shear stress - Clause 1.7.215(C)(4):

$$f_v = \frac{3925000}{2000 \cdot 18} = 109 \text{ MPa}$$

Calculate critical loads

Shear - Clause 1.7.211(B)(2):

$$\lambda_v = 0.8\,\frac{D}{t_d}\sqrt{\frac{F_y}{Ek_v}}$$

$$k_v = 5 + 5/\alpha^2$$

$$\alpha = \frac{\text{width}}{\text{height}} = \frac{975}{2000} = 0.488$$

$$k_v = 5 + \frac{5}{.488^2} = 26.0$$

$$\lambda_v = 0.8 \cdot \frac{2000}{18}\sqrt{\frac{350}{200000 \cdot 26}} = 0.729$$

$$F^{\circ}_{vcr} = [0.58-0.357(\lambda_v-0.58)^{1.18}]\,F_y$$

$$= [0.58-0.357(0.729-0.58)^{1.18}]350 = 190 \text{ MPa}$$

Axial compression - Clause 1.7.211(B)(3):

$$k = (\alpha + 1/\alpha)^2 = \left(0.488 + \frac{1}{0.488}\right)^2 = 6.44$$

$$\lambda = \frac{D}{0.95t_d}\sqrt{\frac{F_y}{Ek}} = \frac{2000}{0.95 \cdot 18}\sqrt{\frac{350}{200000 \cdot 6.44}} = 1.93$$

$$F^{\circ}_{ccr} = \frac{1}{\lambda^2}F_y = \frac{350}{1.93^2} = 94 \text{ MPa}$$

Bending - Clause 1.7.211(B)(3):

$k = 24 + 73\ (2/3-\alpha)^2 = 24 + 73(2/3-0.488)^2 = 26.3$

$$\lambda = \frac{2000}{0.95 \cdot 18} \sqrt{\frac{350}{200000 \cdot 26.3}} = 0.95$$

$$F^{\circ}_{bcr} = [0.072(\lambda-5.62)^2 - 0.78]\ F_y$$

$$= [0.072(0.95-5.62)^2 - 0.78]\ 350 = 276 \text{ MPa}$$

Applied stresses - Clause 1.7.211(B)(4):

$F_{vcr} = 109$ MPa

$$F_{ccr} = \frac{103-40}{2} = 32 \text{ MPa}$$

$$F_{bcr} = \frac{103+40}{2} = 72 \text{ MPa}$$

$$\left(\frac{F_{vcr}}{F^{\circ}_{vcr}}\right)^2 + \left(\frac{F_{bcr}}{F^{\circ}_{bcr}}\right)^2 + \left(\frac{F_{ccr}}{F^{\circ}_{ccr}}\right) < 1.0$$

$$\left(\frac{109}{190}\right)^2 + \left(\frac{72}{276}\right)^2 + \left(\frac{32}{94}\right) = 0.74 < 1.0 \quad \text{therefore OK}$$

Check maximum equivalent stress - Clause 1.7.215(D)(3)

Vertical stress - Clause 1.7.215(C)(2):

$b_{eff} = 2 \cdot 18 t_d = 2 \cdot 18 \cdot 18 = 648\text{mm} > j = 600$ mm

therefore $b_{eff} = 600$ mm

$A = 500 \cdot 30 \cdot 2 + 600 \cdot 18 = 40800$ mm^2

$$\sigma_v = 2 \cdot \frac{3925000}{40800} = 192 \text{ MPa}$$

Horizontal stress - Clause 1.7.215(C)(3):

$$M = 3925 \cdot 0.885 + 3925 \left(\frac{2850-1850}{2 \cdot 2000}\right)\left(1.17-\frac{2.00}{2}\right) = 3640 \text{ kN-m}$$

$$\sigma_n = \frac{3640000}{4531000} \cdot 117 + \frac{3925000}{2 \cdot 70000} \left(\frac{2850-1850}{2 \cdot 2000}\right) = 101 \text{ MPa}$$

Shear stress - Clause 1.7.215(C)(4):

τ = 109 MPa

$f_e = \sqrt{192^2+101^2-192\cdot101+3\cdot109^2}$ = 252 MPa < σ_y = 350 MPa

Check maximum allowable shear - Clause 1.7.210(B)(1):

$$f_{av} = \frac{f_{1w} + f_{2w}}{2} = \frac{103+40}{2} = 72 \text{ MPa}$$

$$V_{max} = 0.58Dt_d\sqrt{350^2 - (2/3f_{av})^2}$$

$$= 0.58\cdot2000\cdot18\sqrt{350^2 - (2/3\cdot72)^2} = 7240 \text{ kN}$$

maximum applied shear = 3925 kN therefore OK

Design load-bearing stiffener

horizontal force = 1.3·250 = 325 kN

vertical force=1.3(1000+350+250+1850)·2 = 6370 kN

b_{eff} = 600 mm A_s = 40800 mm^2

$$I = 2 \cdot \frac{500^3\cdot30}{12} + \frac{600\cdot18^3}{12} = 625291600 \text{ mm}^4$$

$$r^2 = \frac{625291600}{40800} = 15325 \text{ mm}^2$$

e = 88 mm - from design by Interim Design Rules

M = P·e = 6370·.088 = 560 kN-m

Check stability - Clause 1.7.69(B):

$$\frac{P}{.85A_s\cdot F_{cr}} + \frac{MC}{M_u\left(1-\frac{P}{A_sF_e}\right)} < 1.0 \quad C = 0.6$$

$$\left(\frac{kL}{r}\right)^2 = \frac{2000}{15325}^2 = 261$$

$$F_{cr} = F_y\left[1-\frac{F_y}{4\pi^2E}\left(\frac{kL}{r}\right)\right]$$

$$F_{cr} = 350\left[1 - \frac{350}{4\cdot\pi^2\cdot 200000}\right]\cdot 261 = 346 \text{ MPa}$$

$$F_e = \frac{\pi^2 E}{\left(\frac{kL}{r}\right)^2} = \frac{\pi^2\cdot 200000}{261} = 7562 \text{ MPa}$$

$$M_u = S\cdot f_y = 350 \cdot \frac{62529}{25} = 875 \text{ kN-m}$$

$$\frac{6370000}{0.85\cdot 40800\cdot 346} + \frac{0.6\cdot 560000}{875000\left(1-\frac{6370000}{40800\cdot 7562}\right)} = 0.92 < 1.0 \quad \text{therefore OK}$$

Check strength - Clause 1.7.69(B)

$$\frac{P}{0.85A_s F_y} + \frac{M}{M_p} < 1.0$$

$$M_p = 1.5\cdot 875 = 1312 \text{ kN-m}$$

$$\frac{6370000}{0.85\cdot 40800\cdot 350} + \frac{560}{1312} = 0.95 < 1.0 \text{ therefore OK}$$

Check bearing - Clause 1.7.215(D)(2):

$$\frac{6370000}{40800} + \frac{560000\cdot 25}{62529} = 380 \text{ MPa} > 350 \text{ MPa} \quad (9\% \text{ over})$$

Should use slightly larger stiffener

Check required stiffness - Clause 1.7.213(C)(2):

$$I_{T_{req'd}} = \gamma_T^* \frac{Dt_D^3}{12(1-v^2)}$$

$\gamma_T^* = 50$ from Fig. 1.7.213(A)

$$I_{T_{req'd}} = 50 \cdot \frac{2000\cdot 18^3}{12(1-0.3^2)} = 53406600 \text{ mm}^4 < 625290000 \text{ mm}^4 \quad \text{therefore OK}$$

Check torsional buckling strength - Clause 1.7.213(C)(3):

$$\frac{d_s}{t_s} < \frac{0.48}{\sqrt{\frac{F_y}{E}}}$$

$$\frac{250}{30} = 8.3 < \frac{0.48}{\sqrt{\frac{350}{200000}}} = 11.5 \text{ therefore OK}$$

D. SUMMARY

Design by	IDR	TRRL	AASHTO
Total amount of steel (kg)	1230	1040	1135
Total amount of welding (mm)	17000	17000	17000
Stiffeners	load-bearing	load-bearing	load-bearing

RECENT STRUCTURAL ENGINEERING REPORTS

Department of Civil Engineering

University of Alberta

69. *Numerical Analysis of General Shells of Revolution Subjected to Arbitrary Loading* by A.M. Shazly, S.H. Simmonds and D.W. Murray, September 1978.

70. *Concrete Masonry Walls* by M. Hatzinikolas, J. Longworth and J. Warwaruk, September 1978.

71. *Experimental Data for Concrete Masonry Walls* by M. Hatzinikolas, J. Longworth and J. Warwaruk, September 1978.

72. *Fatigue Behaviour of Steel Beams with Welded Details* by G.R. Bardell and G.L. Kulak, September 1978.

73. *Double Angle Beam-Column Connections* by R.M. Lasby and Reidar Bjorhovde, April 1979.

74. *An Effective Uniaxial Tensile Stress-Strain Relationship for Prestressed Concrete* by L. Chitnuyanondh, S. Rizkalla, D.W. Murray and J.G. MacGregor, February 1979.

75. *Interaction Diagrams for Reinforced Masonry* by C. Feeg and J. Warwaruk, April 1979.

76. *Effects of Reinforcement Detailing for Concrete Masonry Columns* by C. Feeg, J. Longworth, and J. Warwaruk, May 1979.

77. *Interaction of Concrete Masonry Bearing Walls and Concrete Floor Slabs* by N. Ferguson, J. Longworth and J. Warwaruk, May 1979.

78. *Analysis of Prestressed Concrete Wall Segments* by B.D.P. Koziak and D.W. Murray, June 1979.

79. *Fatigue Strength of Welded Steel Elements* by M.P. Comeau and G.L. Kulak, October 1979.

80. *Leakage Tests of Wall Segments of Reactor Containments* by S.K. Rizkalla, S.H. Simmonds and J.G. MacGregor, October 1979.

81. *Tests of Wall Segments from Reactor Containments* by S.H. Simmonds, S.H. Rizkalla and J.G. MacGregor, October 1979.

82. *Cracking of Reinforced and Prestressed Concrete Wall Segments* by J.G. MacGregor, S.H. Rizkalla and S.H. Simmonds, October 1979.

83. *Inelastic Behavior of Multistory Steel Frames* by M. El Zanaty, D.W. Murray and R. Bjorhovde, April 1980.

84. *Finite Element Programs for Frame Analysis* by M. El Zanaty and D.W. Murray, April 1980.

85. *Test of a Prestressed Concrete Secondary Containment Structure* by J.G. MacGregor, S.H. Simmonds and S.H. Rizkalla, April 1980.

86. *An Inelastic Analysis of the Gentilly-2 Secondary Containment Structure* by D.W. Murray, C. Wong, S.H. Simmonds and J.G. MacGregor, April 1980.

87. *Nonlinear Analysis of Axisymmetric Reinforced Concrete Structures* by A.A. Elwi and D.W. Murray, May 1980.

88. *Behavior of Prestressed Concrete Containment Structures - A Summary of Findings* by J.G. MacGregor, D.W. Murray, S.H. Simmonds, April 1980.

89. *Deflection of Composite Beams at Service Load* by L. Samantaraya and J. Longworth, June 1980.

90. *Analysis and Design of Stub-Girders* by T.J.E. Zimmerman and R. Bjorhovde, August 1980.

91. *An Investigation of Reinforced Concrete Block Masonry Columns* by G.R. Sturgeon, J. Longworth and J. Warwaruk, September 1980.

92. *An Investigation of Concrete Masonry Wall and Concrete Slab Interaction* by R.M. Pacholok, J. Warwaruk, and J. Longworth, October 1980.

93. *FEPARCS5 - A Finite Element Program for the Analysis of Axisymmetric Reinforced Concrete Structures - Users Manual* by A. Elwi and D.W. Murray, November 1980.

94. *Plastic Design of Reinforced Concrete Slabs* by D.M. Rogowsky and S.H. Simmonds, November 1980.

95. *Local Buckling of W Shaped Used as Columns, Beams, and Beam-Columns* by J.L. Dawe and G.L. Kulak, March 1981.

96. *Dynamic Response of Bridge Piers to Ice Forces*, by E.W. Gordon and C.J. Montgomery, May 1981.

97. *Full-Scale Test of a Composite Truss*, by Reidar Bjorhovde, June 1981.

98. *Design Methods for Steel Box-Girder Support Diaphragms* by Robert J. Ramsay and Reidar Bjorhovde, July 1981.